ORIGINAL RESEARCH ARTICLE

A multi-scale approach to laminated microbial deposits in non-marine carbonate environments through examples of the Cenozoic, north-east Iberian Peninsula, Spain

Concha Arenas-Abad [ID]

Stratigraphy, Science Faculty, IUCA and Geotransfer Group, University of Zaragoza, Zaragoza, Spain

Correspondence
Concha Arenas-Abad, Stratigraphy, Science Faculty, University of Zaragoza, C/ Pedro Cerbuna 12, 50009 Zaragoza, Spain.
Email: carenas@unizar.es

Abstract

This contribution focusses on stromatolites and oncolites as tools to seek diverse environmental and climate information at different temporal scales. The scales are: (a) Low frequency, dealing with macroscopic and megascopic scales, and (b) high frequency, involving calendar and solar frequency bands. Two depositional environments are used for this purpose: (a) Fluvial and fluvial–lacustrine, which can develop under high to moderate gradients, and in low-gradient conditions, and (b) lacustrine, subject to low-gradient, hydrologically closed lake conditions. Several current and ancient examples in the Iberian Peninsula allow high-frequency and low-frequency analyses. Within the wedge-shaped depositional units that fill the high- to moderate-gradient, stepped fluvial systems, stromatolites form half domes and lenticular bodies, commonly at the wedge front. Oncolites are uncommon. These stromatolites developed in moderate to fast-flowing water in stepped cascades and rapids. Their geometry and extent reflect the topography of the bedrock and later ongoing growth. In low-gradient fluvial and fluvial-(open) lacustrine systems the depositional units are tabular, low-angle wedge-shaped and lenticular and have great spatial facies variability. The dominant oncoid and coated-stem limestones form gently lenticular stacked bodies, developed in wide, low to high-sinuosity channels within wide tufaceous palustrine areas and small lakes. In the Ebro Basin saline carbonate lacustrine systems, stromatolites form thin planar to domed and stratiform bodies and are associated with muddy-grainy laminated carbonates and very rare oncolites, together forming ramp-shaped units that represent the inner fringes of high lake-level deposits. This geometry reflects low-gradient lake surface and shallow water conditions. Textural and structural features allow different ranks of laminae and types of lamination to be distinguished. Texture, together with the $\delta^{13}C$ and $\delta^{18}O$ values of consecutive laminae, are useful in distinguishing environmental and climate changes operating over different time spans. Periodicity analysis of lamination can help to discern any temporal significance in the lamination.

1 | INTRODUCTION

Laminated microbial deposits form in various depositional settings within marine and non-marine environments. In non-marine environments, these deposits comprise diverse tufa, speleothem and travertine facies, stromatolites and oncolites. Travertine and speleothem deposits are not included in this study due to the specific conditions under which they form, which are clearly different with respect to those of microbial facies formed in surface meteoric environments. The study of these laminated microbial facies has been the focus of many works from a variety of perspectives and scales, involving the use of different proxies, such as geochemistry of lamination (Andrews et al., 1997; Anzalone et al., 2007; Arenas et al., 2019; Dabkowski et al., 2015; Zamarreño et al., 1997), geochemistry of different facies (Andrews et al., 1997; Arenas et al., 2000) and periodicity of lamination (Pérez-Rivarés et al., 2019; Storrie-Lombardi & Awramik, 2006; Tang et al., 2014). However, focussing on sedimentology, investigations are commonly centered on a single approach, either the lamination or the sedimentary facies (Lettéron et al., 2018; Seard et al., 2013), with the aim of interpreting the depositional, hydrological or climate conditions over these two disparate time scales. Therefore other attributes that also deserve attention are not included in these studies, for example, the geometry of the microbial-bearing sedimentary bodies, the position of microbialites in the facies associations (FA; i.e. simple vertical sequences or cycles), the integration of microbialites in the sedimentary facies models as indicators of the spatial and temporal evolution of the depositional systems and their significance as reservoir analogs (Della Porta, 2015; Harris et al., 2013; Muniz & Bosence, 2015).

Microbial lamination can be observed at different scales, making its interpretation complex, either environmental (depositional characters, type of sediment, depth, energy and chemical composition of water), climate (temperature, precipitation and evaporation) or temporal significance (Hofmann, 1973; Petryshyn et al., 2012; Storrie-Lombardi & Awramik, 2006).

The focus of this contribution is on laminated microbial deposits in fluvial and lacustrine carbonate environments, in particular stromatolites and oncolites, and their relationships with other lithofacies, as tools to gather varied information, primarily environmental (i.e. depositional characters, type of sediment, depth, energy and chemical composition of water) and climate, at different temporal scales. To achieve this

purpose three types of sedimentary systems with a wide array of carbonate facies in the north-east Iberian Peninsula are compared (fluvial, fluvial–lacustrine and saline lacustrine environments). In each case, the laminated microbial deposits form distinct 3D bodies within the sedimentary units, and occur at specific positions in the vertical FA, allowing the environmental and hydrological significance to be inferred at macroscopic scale and expressed through conceptual facies models. Indeed, the environmental, climate and temporal significance of lamination is discussed from a multi-proxy approach to these examples.
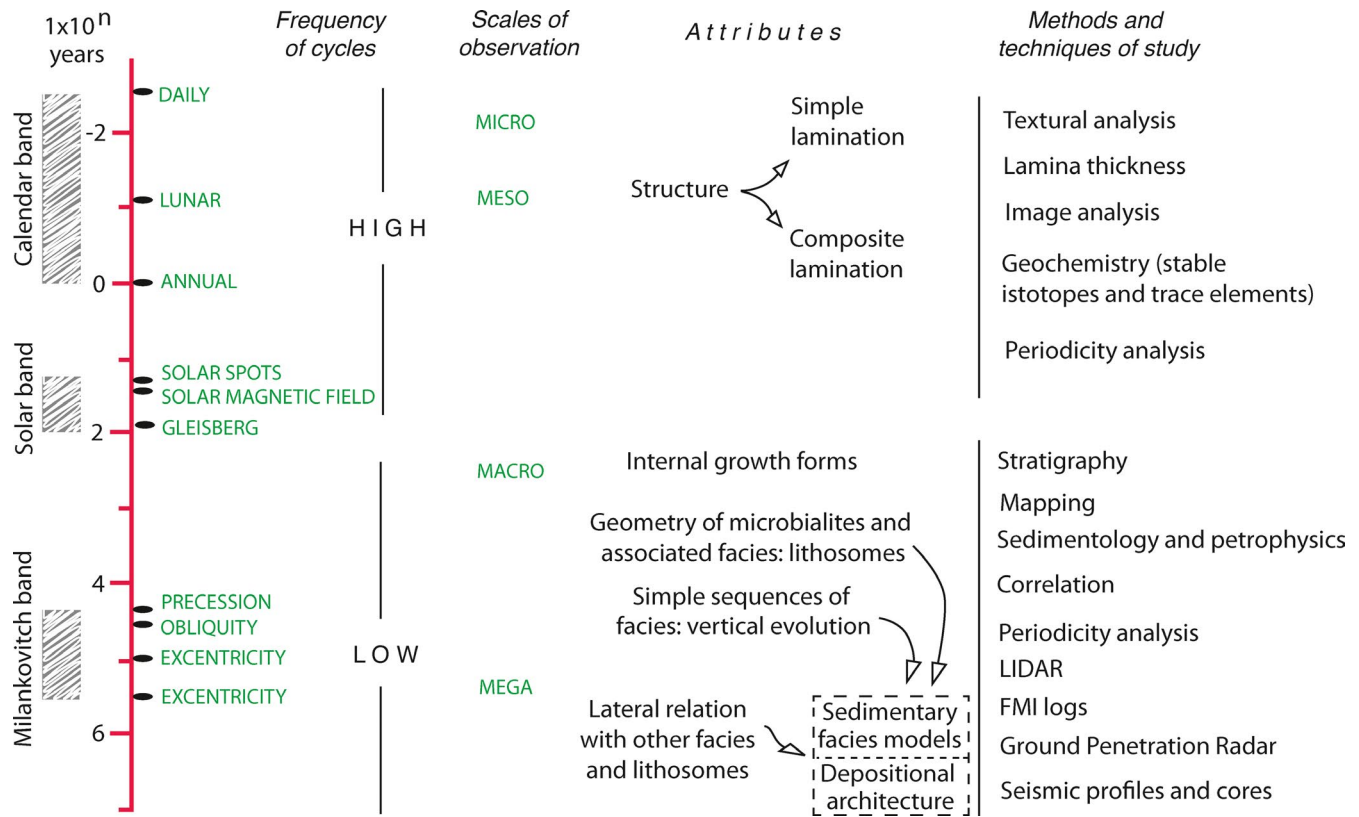
1.1 | Scales of observation of microbialite attributes and type of information

The scales of observation and study of laminated microbial deposits vary from microscopic to megascopic and, when referred to the duration of the related cycles, span calendar, solar and Milankovitch frequencies (Figure 1). Based on frequency or duration, the relevant cycles can be grouped into:

1. High frequency, involving calendar and solar frequencies, which refers to microscopic and mesoscopic scales. The relevant microbialite characters deal with lamination and laminae (vertical arrangement of laminae, either simple or composite laminae, and shape, thickness and other characteristics of the laminae).
2. Low frequency, including Milankovitch cycles, dealing with macroscopic and megascopic scales. The relevant characteristics are diverse and include the microbialite internal growth forms, the geometry of the microbialitic lithosomes and the relationships with other lithofacies, and the position of the microbialites in vertical FA.

Therefore, it is possible to gather environmental information from the spatial and temporal distribution of microbialites in sedimentary systems (i.e. from their lateral and vertical relationships with other facies) and climate information (including hydrology) at different scales, from the lamination, the internal growth forms and different properties of the stromatolitic bodies. Ultimately the information will depend on the methods and analytical techniques used in each case, selected according to the spatial and temporal scales of study (Figure 1).

The examples that are considered in this paper allow for a discussion of the environment and climate based on:

FIGURE 1 Frequency bands of the periodic cyclic sedimentation from Fischer and Herbert (1986), their relationship with common methods and techniques and the characteristics of microbialites studied at each scale of observation. FMI log: Fullbore Formation Micro Imager log

1. Geometry of the microbialite bodies and their relationship with other lithofacies.
2. FAs: position of the microbial deposits, erosional or non-erosional relationships, and any other sedimentological characteristics.
3. Lamination and laminae: arrangement and types of laminae.

Points 1 and 2 provide knowledge on hydrodynamics, water level changes, depositional architecture, and ultimately allows the proposal of facies models. Point 3 allows for high-resolution interpretation of changing environment and climate parameters, and discussion on temporal significance of lamination.

The factors that control the geometry of the sedimentary fill and its spatial–temporal evolution are approached by comparing several known basins. Likewise, the factors involved in high-frequency sedimentary and geochemical cyclicity are also exposed through the several cases considered.

2 | NON-MARINE LAMINATED MICROBIALITE-BEARING SYSTEMS

Among the possible cases, the depositional environments with laminated microbialites that are discussed here are:

1. Fluvial and fluvial–lacustrine systems, which depending on the slope of the sedimentation area can develop in high-gradient to moderate-gradient conditions, and in low-gradient conditions.
2. Lacustrine systems, with low-gradient, hydrologically closed lake conditions.

These depositional contexts generate a specific geometry in the units that fill the basins and produce different features in the associated microbial deposits. The detailed examples considered here are: Quaternary fluvial systems in the Iberian Range, Upper Miocene fluvial–lacustrine systems in the Ebro Basin, and early to middle Miocene lacustrine systems in the Ebro Basin (Figure 2).

2.1 | High-gradient to moderate-gradient fluvial systems

2.1.1 | Depositional geometry, architecture and facies models

These fluvial systems develop in narrow areas, that is, valleys commonly a hectometre up to a few kilometres wide and a few to tens of kilometres long. Typically these carbonate-dominated, high to moderate-gradient fluvial systems form
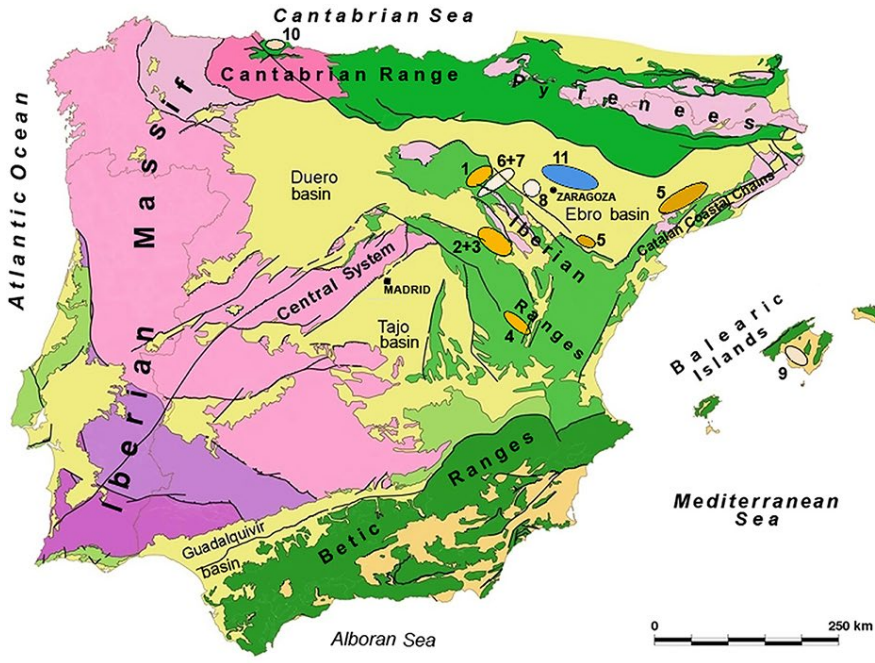
FIGURE 2 Location of some examples of sedimentary systems mentioned in the text. 1: Añamaza river valley; 2 and 3: Mesa and Piedra river valleys; 4: Ebrón river valley; 5, 7, 8 and 11: Ebro Basin. 5: Alcorisa (south) and Vilanova de Prades-Igualada-Monserrat (east); 7: Borja; 8: Montolar hill; 6: Añamaza, on the Iberian Range close to the Ebro Basin boundary; 9: Mallorca Basin (Cala Blanca Formation); 10: Asturias (Vega Formation); 11: Sierra de Alcubierre and Montes de Castejón (genetic stratigraphic units T5, T6 and T7). Geological map adapted from Vera (2004)
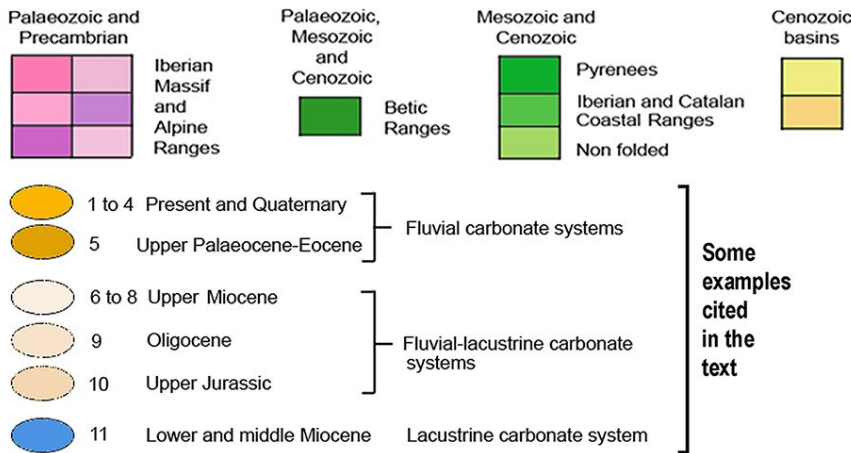
along stepped longitudinal profiles, with several knickpoints along the main water course/s, and with much smaller development on the valley sides, that is, through transversal sections (Arenas-Abad et al., 2010; Ford & Pedley, 1996, and references therein). The slope of modern systems that fit the high to moderate-gradient settings ranges from 1% to 2%; although within some stretches the slope can be higher (Arenas et al., 2015a). Generally, water that feeds these systems comes from karstic springs (Capezzuoli et al., 2010; Durán, 1989; Pentecost, 2005; Sancho et al., 2015). Calcium carbonate precipitation, primarily calcite, occurs once the saturation level of the mineral is reached, which commonly takes places at some distance from the spring, after CO_2 loss and equilibration with atmosphere (Auqué et al., 2013, 2014; Ordóñez et al., 2016).

The depositional units that fill the valleys are lenticular and wedge-shaped bodies that thicken downstream (i.e. in longitudinal sections) and have lenticular or channel-like transverse sections (Figure 3). Generally, within each body, facies distribution through space corresponds to moss boundstones, stromatolites and down-growing stem boundstones, formed in cascade and barrage-cascade environments, and phytoclast rudstone and packstone, bioclastic limestones, carbonate sands and silts, and up-growing stem boundstones formed in gently sloping channel and pool environments upstream of the barrages.

Basically, there are two main geometrical types (Figure 3): small wedges, in high-slope stretches (Figure 3A,B) and large wedges, in moderate-slope stretches (Figure 3C). In both types, stromatolites are dominant at the downstream portions of the wedges, along with moss and hanging-plant boundstones, which typically correspond to the cascade or barrage-cascade environment (Arenas et al., 2014b). Within the wedges, moss boundstones and stromatolites form half domes and lenticular bodies, with moderate to highly inclined beds and layers (Figure 4A,B). Decreasing the slope
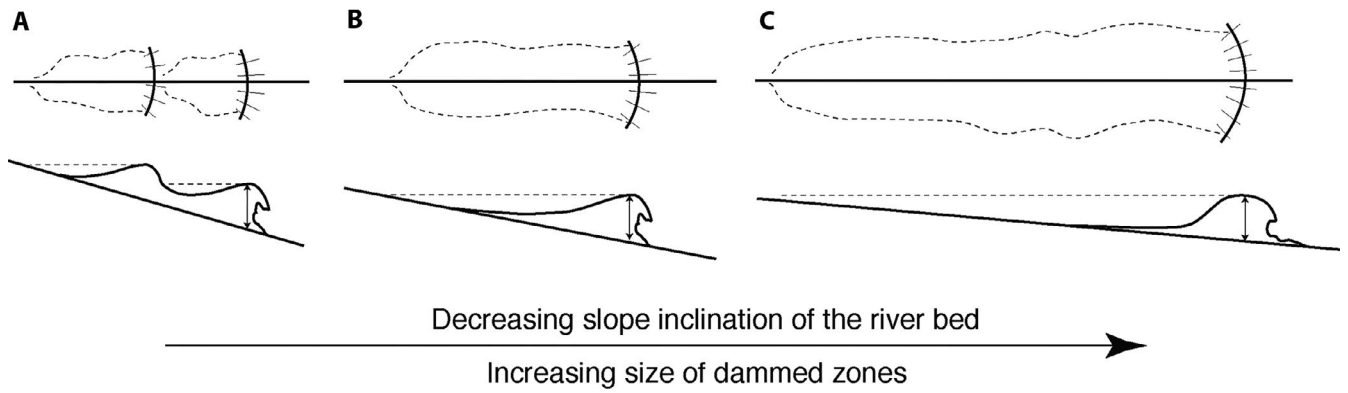
FIGURE 3 Plan view of development of barrage-cascade and associated dam environments and cross-sections (wedge-shaped bodies) along flow, as a function of the riverbed gradient. Decreasing gradient from A to C. Steep gradients produce higher and narrower barrages and shallower gradients are associated with more robust barrages. Stromatolites form at the front of the wedges. From Vázquez-Urbez et al. (2012), reproduced with permission of John Wiley and Sons
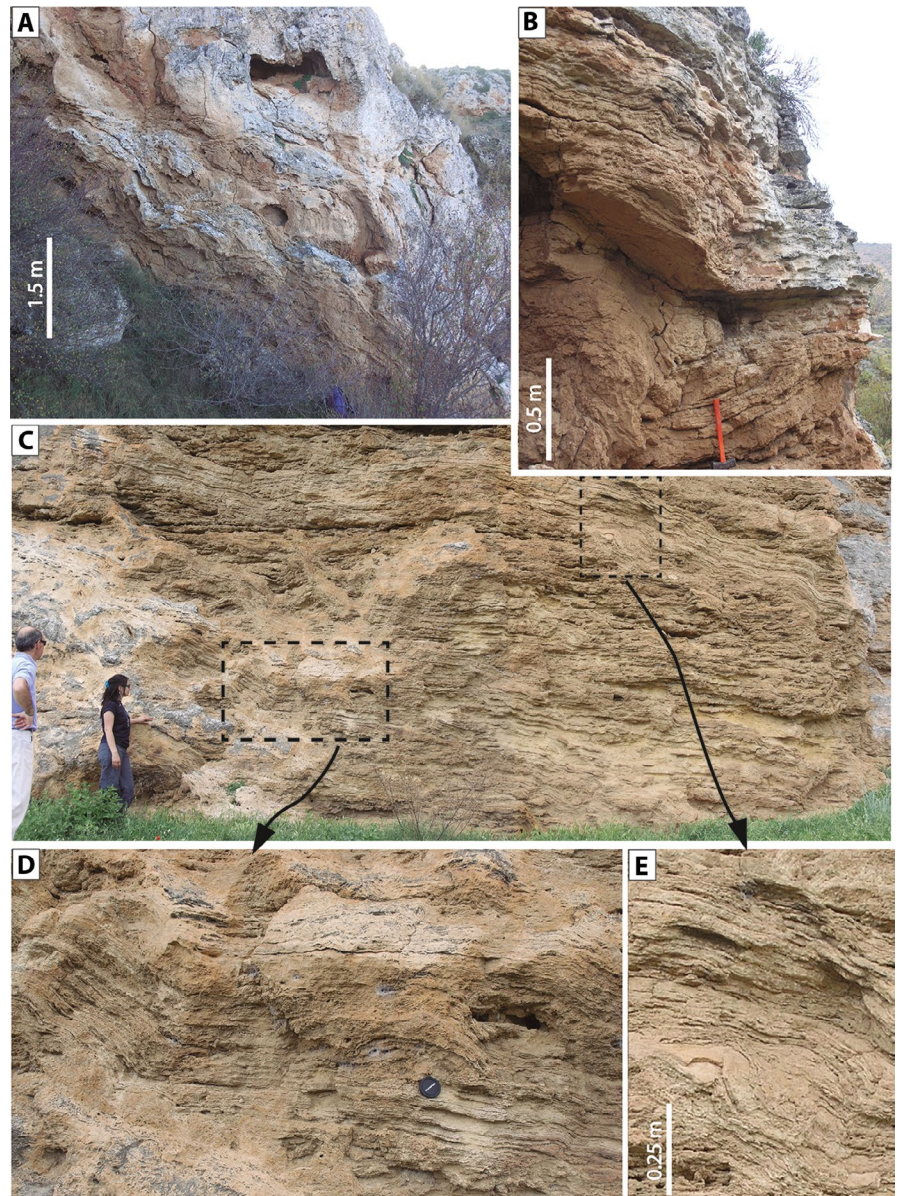
FIGURE 4 Geometry and details of stromatolites formed in high-gradient and moderate-gradient fluvial systems. (A and B) Half domes and highly inclined bodies, formed at the front of a complex wedge-shaped unit; River Añamaza, Pleistocene (MIS 5). (C–E) Gently inclined stromatolite deposits including patches of phytoclast rudstones and moss boundstones; (D and E) details of lamination; Mesa River, Pleistocene (MIS 5). Lens cap for scale

of the river bed results in an increase in the length of these wedge-shaped bodies, allowing more extensive deposits of the dam and gently-sloping channel zones to form (Figure 3; Vázquez-Urbez et al., 2012). In some cases, moderate-slope stretches between knickpoints are sites for extensive stromatolite development close to the downstream knickpoint (Figure 4C,D,E). In contrast, in steep slope stretches along the valleys, erosion has more impact, and multistorey wedges consisting of several lenticular and wedge-shaped bodies that are separated by erosional features are common (Figure 5A). Generally, these deposits consist of alternating moss boundstones and stromatolitic bodies, which include patches of down-growing stem boundstones and phytoclast rudstones (Figure 6A). Generally, in the wedges, as a result of the progradation of the cascade front, the upstream dam facies appear on former stromatolite and moss deposits formed at the cascade front; at the same time, the latter facies pass laterally into the downstream dam facies (Figure 5).

FAs show that the most common environmental situations involving stromatolites are:

1. Free-flowing water channels and cascade and barrage-cascade environments, after filling of the active channel by coarse detrital sediments and phytoclast accumulations, stromatolite facies formed in stretches where rapid flow occurs. On occasion, the latter are laterally related to moss boundstones (e.g. FA 2; Figure 5A).
2. Small cascade and barrage-cascade environments, mainly consisting of moss mounds and stromatolite facies, laterally related to carbonate sand and lime mud and up-growing stem boundstones (e.g. FA 3; Figure 5B).

One of the best examples that record both high-gradient and moderate-gradient conditions is the Quaternary Añamaza Valley, with Holocene and Pleistocene records, in the Iberian Range (Arenas et al., 2014b). The sedimentary facies model for the high-gradient conditions shows small wedge-shaped multistory wedges, up to 70 m thick, with abundant moss boundstones and stromatolites, mainly at the front of the wedges, and also phytoclastic rudstones, together forming highly inclined, lenticular and half dome deposits (Figures 4A and 5A). In contrast, in the moderate-slope conditions the units are large wedges dominated by carbonate silts and sand, bioclastic limestones, marls and fine-phytoclast rudstones in the pools, small oncoids in areas of slow-flowing water, and moss boundstones and stromatolites in the shallow cascades and rapids (Figures 4C and 5B).

Similar situations and facies models are depicted for other Quaternary stepped fluvial systems, as in the case of the Mesa, Piedra and Ebrón river valleys, in which stromatolites constitute extensive and thick deposits formed in fast to moderate water flow (Figures 4B and 6A). Other examples have been studied by Violante et al. (1994), Ordóñez et al.

(2005), Carthew et al. (2006), Özkul et al. (2014), Martini and Capezzuoli (2014) and Toker (2017). These models are generally complex because of the great variability and mobility of the different environments involved, the presence of several stages of deposition and other peculiar features that are present in some cases (e.g. diffluence episodes, as in the River Piedra; Vázquez-Urbez et al., 2011, 2012; transverse filling of a main fluvial system, in southern Spain, García-García et al., 2014).

## 2.1.2 | Structure, texture and stable isotopes

The most abundant laminated microbial structures in high to moderate-gradient conditions are stromatolites and plant coatings (i.e. preserved as stem rudstones and down-growing stem boundstones, and less common up-growing stem boundstones; Figure 6C). Within the stromatolite bodies it is not uncommon to find centimetre-thick interbeds consisting of phytoclast rudstone, moss boundstone or down-growing stem boundstone (Figure 6A). The thickness of the stromatolites is highly variable and can reach up to several metres, which enables detailed and continuous sampling over extended intervals (Figure 4D,E).

Focussing on stromatolites, in some Pleistocene and Holocene fluvial systems studied in north-eastern Spain, lamination consists of convex to slightly wavy to flat laminae, generally very continuous in outcrop with wavy to smooth profiles in cross-sections (Figure 6B,D).
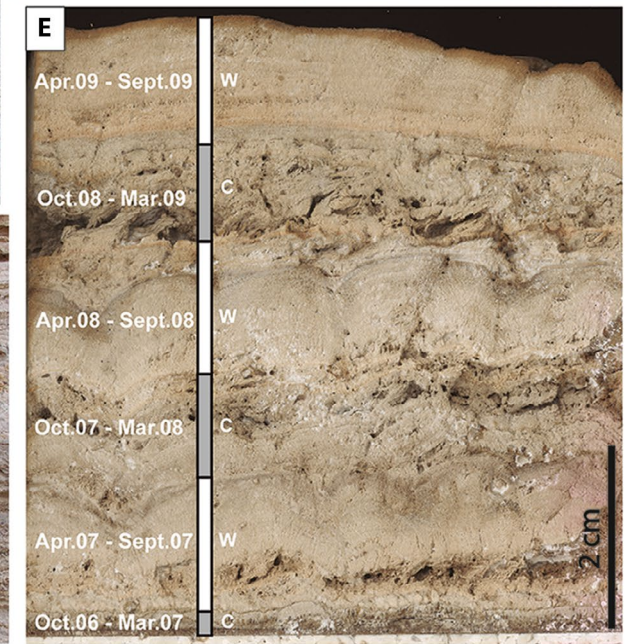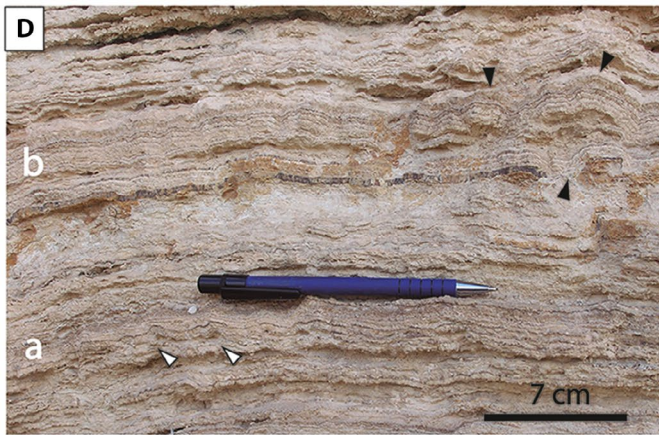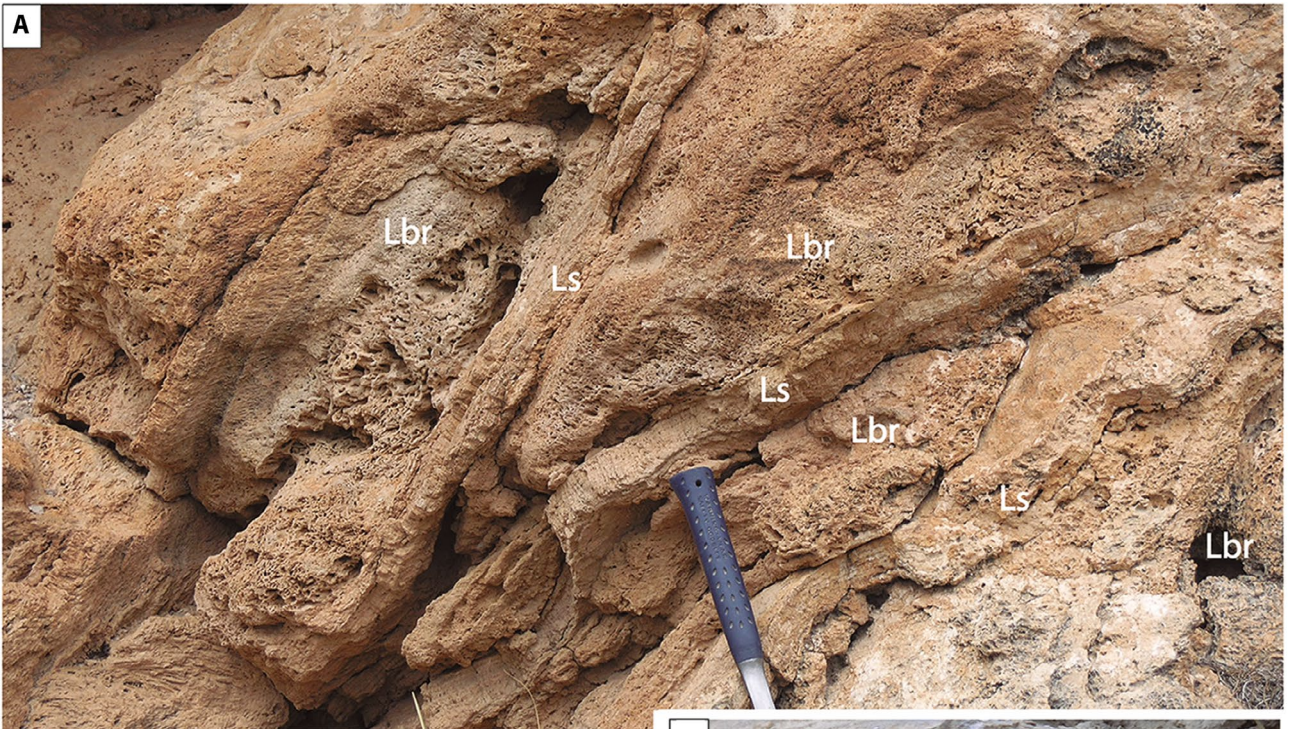
Microscopically, these stromatolites are formed of two main types of laminae that alternate through time: thick, small-crystal laminae and thin, large-crystal laminae (Figure 7A,B). The small crystals are close to isodiametric, forming micrite to microsparite textures; the large crystals tend to be elongated, with the long axes perpendicular to lamination. Both types of laminae contain microbial evidence, primarily cyanobacterial filaments, which in most cases are preserved as calcite tubes (Figure 7C,D). In detail, the laminae are smooth to highly wavy, in many cases as a result of the palisade, fan or shrub-like shapes of the microbial filamentous structures (Figure 7B,C). Generally, porosity is higher in the small-crystal laminae when compared to the large-crystal laminae, being dominant in the frame-growth and vug types. However, porosity features can be highly variable depending on the studied systems (Arenas & Jones, 2017).

The example of the River Añamaza lamination
In the Añamaza river valley (north-west Iberian Range, Spain), lamination in Pleistocene (Marine Isotope Stages MIS 5 and 6) and Holocene stromatolites (MIS 1) (detailed dating in Sancho et al., 2015), consists of flat to slightly undulate, locally domed, laminae. The Pleistocene stromatolites developed at the downstream part of a small wedge along
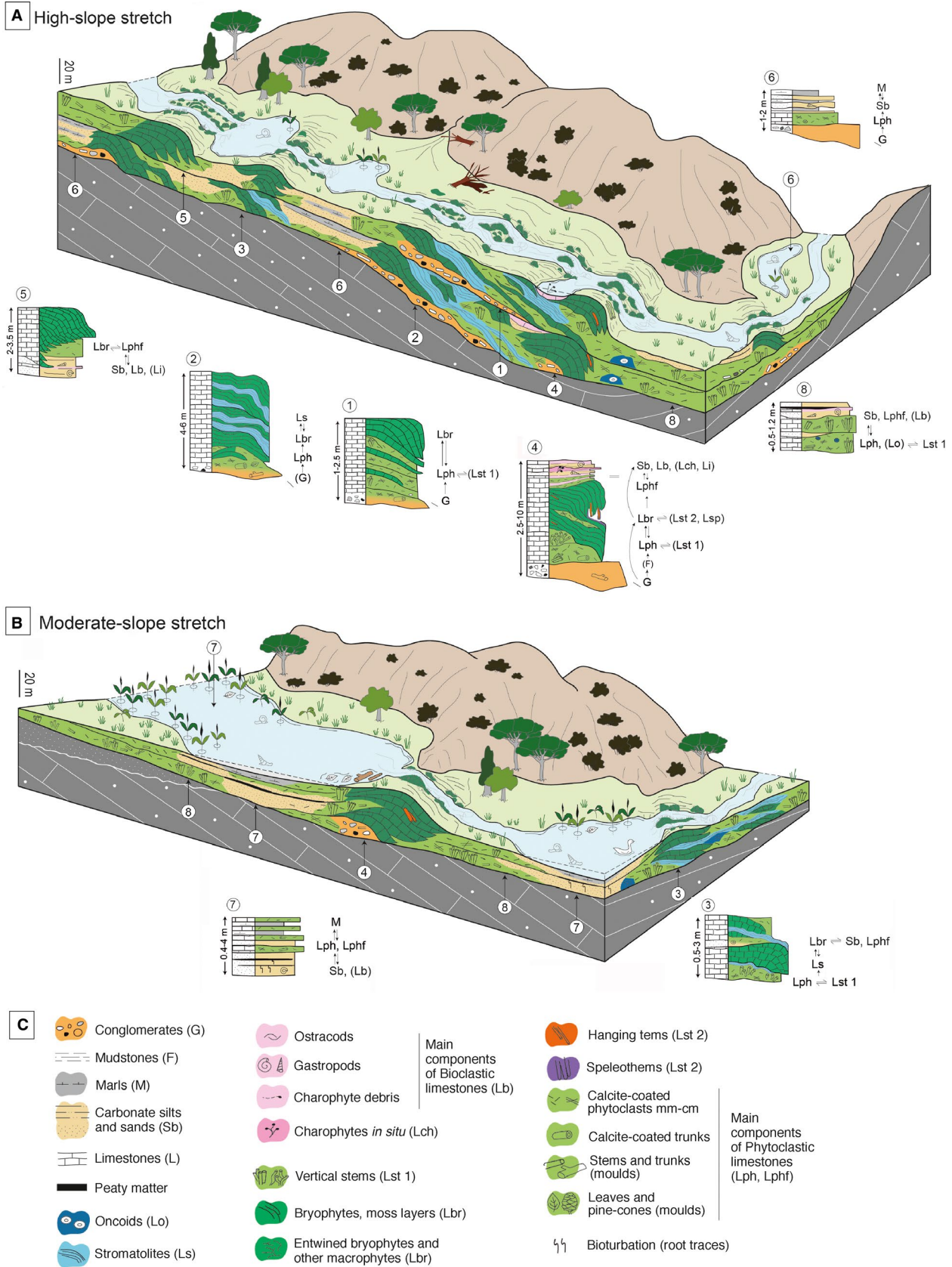
FIGURE 5 (A and B) Sedimentation models proposed for high-slope (A) and moderate-slope stretches (B) of the Pleistocene and Holocene deposits of the Añamaza river valley, indicating the common FA. Note stromatolites dominate in high-slope stretches and rapids of both models. (C) Legend of symbols used in A and B. Adapted from Arenas et al. (2014b); reproduced with permission of John Wiley and Sons

A — Lbr, Ls, Lbr, Ls, Lbr, Ls, Lbr

B — Lph, Ls, 10 cm

C — 5 cm

D — b, a, 7 cm

E — Apr.09 – Sept.09 W, Oct.08 – Mar.09 C, Apr.08 – Sept.08 W, Oct.07 – Mar.08 C, Apr.07 – Sept.07 W, Oct.06 – Mar.07 C, 2 cm

FIGURE 6 Field views (A–D) and hand sample cross-section (E) of laminated microbialites formed in high-gradient fluvial systems. (A) Alternating stromatolite (Ls) and moss boundstone layers (Lbr) in a half dome body developed in a cascade-barrage, River Piedra, Pleistocene. Hammer handle for scale. (B) Detail of stromatolite lamination (Ls) and associated fine phytoclast rudstone (Lph), River Añamaza, Pleistocene (MIS 6). (C) Laminated microbialite formed around a trunk. Note undulate lamination at the base. River Añamaza, Pleistocene. (D) Detail of lamination formed on a slightly inclined surface. Note wavy laminae oriented parallel to flow (arrows in layer a) and small domes (arrows in layer b). River Ebrón, Pleistocene (MIS 5). (E) Stromatolite deposit formed on an artificial substrate installed on a small stepped cascade in the River Piedra, with identification of deposits accumulated over a six-month period, resulting from periodic measurements from October 2006 to September 2009 (data in Arenas et al., 2014a). MIS: Marine Isotope Stages

a high-slope area of the valley (Arenas et al., 2014b). The Holocene stromatolites formed at the downstream part of a large wedge, in a moderate-slope area of the valley that included small barrages and cascades and wide palustrine zones (Arenas et al., 2014b).

Lamination in all studied specimens results from alternating micrite and spar calcite laminae (1–3.5 mm thick) with abundant cyanobacterial filamentous bodies that are arranged as adjacent bush or fan-shaped bodies forming palisades, and large-crystal calcite laminae (0.2–1 mm thick), in which the crystals (up to 0.5 mm long) are set perpendicular to lamination and occur on top of the small-crystal laminae (Figure 7C). Both sharp and gradual boundaries between these types of laminae can be found (Osácar Soriano et al., 2017).

The $\delta^{18}O$ values of successive laminae in these examples show a cyclic pattern through time, with the large-crystal laminae having significantly less negative values than the small-crystal laminae (Table 1). Differences between the mean $\delta^{18}O$ values of the two types of laminae decrease with time (0.94 and 0.51‰ in the Pleistocene and 0.21‰ in the Holocene) (Osácar Soriano et al., 2017). The $\delta^{13}C$ values of the large-crystal laminae are slightly more negative than those of the small-crystal laminae, but there is not a clear pattern of variation through time. The mean differences between the two types of laminae are very small in the Pleistocene samples (0.11 and 0.01‰) and slightly higher in the Holocene (0.36‰) (Osácar Soriano et al., 2017).

An example of lamination in the River Piedra
The River Piedra (central Iberian Range, Spain, Figure 2) allows Pleistocene stromatolites and currently forming stromatolites to be compared in the same river, both in small cascades. The comparison is more representative in the River Piedra than in other Iberian rivers because of the long available record of recent stromatolites, spanning 13 years (Arenas et al., 2014a).

A present-day stromatolite formed on an artificial substrate, installed on a small cascade and monitored every 3 and 6 months from 2000 to 2012 (Arenas et al., 2014a), was used for the comparison (Arenas et al., 2019). At that site, the mean sedimentation rate measured over 13 years was 16 mm/year. Each millimetre to 2 cm thick unit measured during the periodic monitoring (Figure 6E) corresponds to

6-month warm and 6-month cool periods (i.e. spring and summer, and autumn and winter). In detail, each of these intervals is formed of dominantly dense composite laminae and dominantly porous composite laminae, both having cyanobacterial filaments, preserved as calcite tubes forming palisades (Figure 7E,F; Arenas & Jones, 2017). Based on known, seasonally measured water $\delta^{18}O$ values, the $\delta^{18}O$ values of these warm-period and cool-period deposits provided temperature estimates very close to water temperatures measured during the corresponding periods (Table 1). Moreover, stable isotopes from high-resolution sampling of a piece of this modern stromatolite yield very good agreement between calculated and measured temperatures (Arenas et al., 2018).

The ancient sample used for comparison was a Pleistocene stromatolite at the site of Los Bancales (a lateral deposit of the River Piedra formed during diffluence; see Vázquez-Urbez et al., 2011). The above-mentioned two types of alternating laminae—with small crystals and with large crystals—are present. Cyanobacterial filaments forming fan-shaped and bush-shaped bodies are abundant in the small-crystal laminae (Figure 7A,B). The stable isotope values of samples taken in consecutive laminae (one or two samples per lamina) in the Pleistocene stromatolite yielded an irregular pattern for $\delta^{13}C$ values. In contrast, $\delta^{18}O$ values showed a cyclic variation, in which the large-crystal laminae have less negative values, representing lower water temperature, and the small-crystal laminae have more negative values, representing higher water temperature (Table 1). The calculated Tw difference between these two types of laminae is 7–8.1°C. Assuming each pair formed in a year, the sedimentation rate was 8.3 mm/year (Arenas et al., 2019).

2.2 | Low-gradient fluvial and fluvial–open lacustrine systems

2.2.1 | Depositional geometry, architecture and facies models

Fluvial and fluvial–open lacustrine carbonate systems that develop in low-gradient, non-stepped conditions vary in extent, but commonly occur in wide transverse sections (i.e. tens of kilometres wide across the main current direction). These low-gradient systems develop in a variety of geodynamic settings, involving foreland, rift and semi-graben basins (Arenas
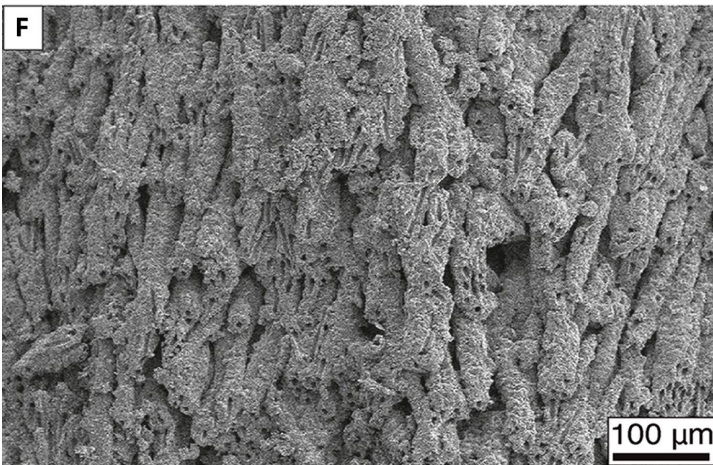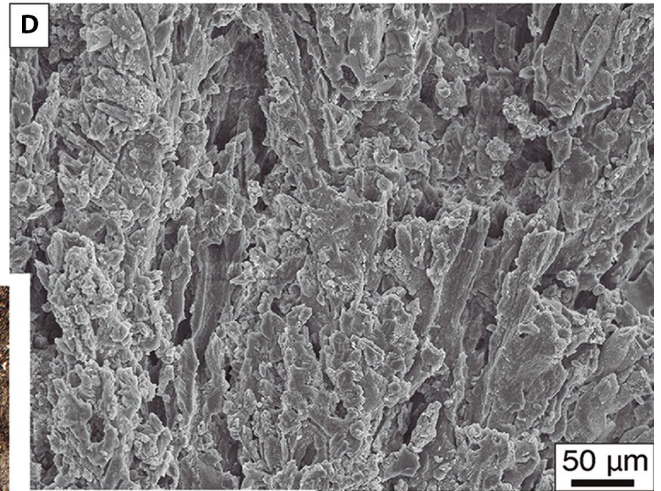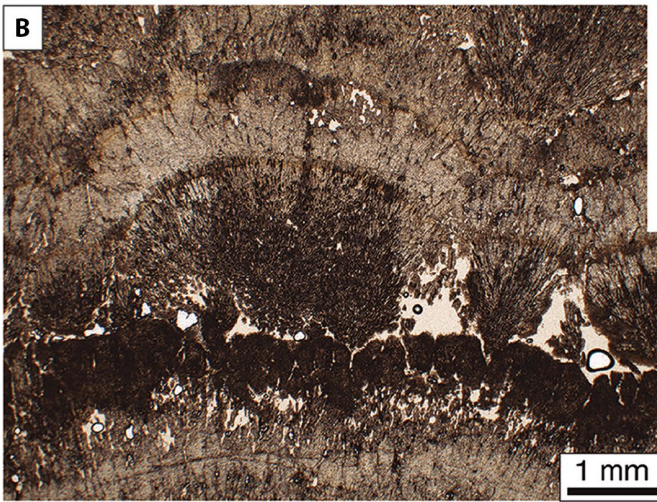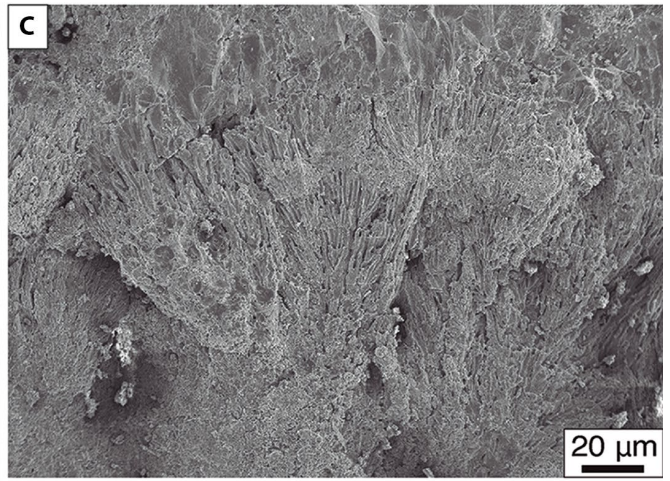
FIGURE 7 Photomicrographs of lamination, texture and microbial components of stromatolites formed in high and moderate fluvial carbonate systems. (A and B) Small and large-crystal laminae containing or evoking cyanobacterial filaments arranged in fan-shaped bodies. River Piedra, Los Bancales, Pleistocene, MIS 6-7. (C and D) Scanning Electron Microscope (SEM), River Añamaza, Pleistocene. (C) Adjacent fan-shaped bodies consisting of calcite tubes formed by calcite precipitation on cyanobacterial filaments; note larger crystals at top. (D) Detail of tubes and filament moulds. (E and F) Recent deposit of the base of Figure 6E. (E) Lamination disrupted by erosion at top. Note macrocrystal laminae at the base. (F) Calcite tubes from cyanobacterial filaments forming a palisade. Image in C from Arenas et al. (2014b), reproduced with permission of John Wiley and Sons

TABLE 1 Stable isotope values ($\delta^{13}C$ and $\delta^{18}O$‰ V-PDB) of light/porous and dark/dense laminae in different fluvial stromatolites, fluvial oncolites and lacustrine stromatolites. Añamaza River values from Osácar Soriano et al. (2017), Piedra River values from Arenas et al. (2019), Upper Jurassic values from Arenas et al. (2015b) and Ebro Basin values from Martín-Bello et al. (2019b). For details on calculation of water temperature, refer to the corresponding reference

Stromatolites (Ls) and oncolites (Lo); age, specimens and samples	$\delta^{13}C$ ‰ (V-PDB)	$\delta^{18}O$‰ (V-PDB)	Calculated mean difference in Tw (ºC)
Añamaza River (Ls)			
Holocene (N = 23)			
Light/porous lam. (N = 14)	−4.92	−8.08	0.9
Dark/dense lam. (N = 9)	−5.28	−7.87	
Pleistocene (MIS 5; N = 30)			
Light/porous lam. (N = 15)	−6.03	−8.84	2.1
Dark/dense lam. (N = 15)	−6.02	−8.33	
Pleistocene (MIS 6; N = 26)			
Light/porous lam. (N = 13)	−6.14	−8.46	4
Dark/dense lam. (N = 13)	−6.03	−7.52	
Piedra river (Ls)			
Present River (P-14; Oct 2000 to Sept 2012; N = 24)			
Porous—6-month cool period	−7.84	−7.75	4.0–4.2
Dense—6-month warm period	−8.00	−8.65	
Middle Pleistocene (LB-9a; N = 33)			
Light/porous lam. (N = 17)	−7.14	−7.29	7.6–8.1
Dark/dense lam. (N = 16)	−7.02	−8.97	
Middle Pleistocene (LB-9b; N = 24)			
Light/porous lam. (N = 12)	−7.13	−7.66	7.0–7.4
Dark/dense lam. (N = 12)	−7.33	−9.15	
Jurassic (Lo)			
Upper Jurassic oncoids			
Light/porous laminae (N = 17)	−6.36	−4.87	—
Dark/dense laminae (N = 19)	−6.06	−4.76	—
Ebro Basin (Ls)			
Lower and middle Miocene, T7 (N = 15)			
Light/porous laminae	−4.23	−6.23	—
Dark/dense laminae	−4.4	−5.93	—
Lower and middle Miocene, T6 (N = 80)			
Light/porous laminae	−1.21	−3.87	—
Dark/dense laminae	−1.05	−3.65	—
Lower and middle Miocene, T5 (N = 79)			
Light/porous laminae	−1.58	−3.95	—
Dark/dense laminae	−1.38	−3.57	—

et al., 2000, 2015b; Leinfelder, 1985; Parcerisa et al., 2006; Talanda et al., 2017; Zamarreño et al., 1997).

The geometry of the microbialite-bearing sedimentary units that fill the basin is varied: tabular, lenticular and ramp-like (low-angle wedges), in sections parallel to the sediment input direction (Figure 8). In these systems, oncoid and phytoclast-bearing channel facies and tuffaceous paludal facies are dominant, primarily upstream and/or close to the main water source; different lacustrine facies containing various components (molluscs, ostracods, charophytes, coal, etc.) can be dominant downstream. Stromatolites are not abundant and commonly are limited to local, thin bodies. Nonetheless, the spatial distribution of the above-mentioned environments may be highly variable and, typically, facies distribution shows rapid changes through space (Arenas et al., 2007; Capezzuoli et al., 2014).

### The upper Miocene last filling stage in the Ebro Basin

A low-gradient, non-stepped fluvial–lacustrine system occurred in the Upper Miocene during the last filling stages of the Ebro Basin, namely genetic stratigraphic unit T8, Tortonian to unknown age (Muñoz et al., 2002; Vázquez-Urbez et al., 2013). In the area of Borja (Figure 2), this unit is 40–55 m thick and consists of coarse and fine fluvial detrital deposits at the base that grade upward into a sequence dominated by limestones. These limestone facies of the Neogene of the Ebro Basin are unique: mostly oncoid rudstones, phytoclast rudstones and a variety of bioclastic limestones (gastropod and ostracod mudstones and wackestones), with less common interbedded up-growing stem boundstones, rare stromatolites and marls. The geometry of the carbonate deposits is tabular and low-angle wedge-shaped and lenticular (Figures 8 and 9), with great spatial and temporal variability of facies and corresponding environments (Váquez-Urbez, 2008).

The sedimentary facies model for unit 8 in the Borja area corresponds to a fluvial–lacustrine–palustrine, hydrologically open system (Vázquez-Urbez et al., 2013; Figure 10). Low-sinuosity and minor high-sinuosity oncoid and phytoclast channels, interchannel extensive palustrine areas and ponded areas, in which hydrophilous plants and diverse molluscs thrived, were connected to a lake downstream. In the lake, gastropod, ostracod and charophyte limestones and marls formed, as well as oncoid rudstones. The oncoid and/or phytoclast facies occur at the base of the simple sedimentary sequences, at places showing erosional bases (Figure 10; FA 3a,b, 10a,b, 11a,b). Stromatolites are rare and form centimetre-thick flat to slightly domed bodies, associated with some oncoid deposits (Figure 10; FA 10a). The dominant oncoid and coated-stem limestones form low-angle lenticular stacked bodies (Figure 11A) laterally and vertically related to tabular and lenticular bioclastic limestone bodies; aggradation was the main process throughout.

Other examples

Other close examples occur in the Miocene of the Añamaza area (north-west Iberian Range, close to the south-western boundary with the Ebro Basin, Figure 2), in which the fluvial sedimentary units form metre-thick lenticular, convex-up and wedge-shaped bodies, mostly formed of phytoclast and minor oncoid rudstones (Figure 9C). The wedge-shaped bodies are gently inclined in the flow direction or basinward (i.e. eastward and north-eastward).

In the central part of the Ebro Basin, genetic stratigraphic unit T8 in the Montolar hill area (Figure 2) is an excellent example of thick lenticular bodies, mostly formed of oncoids, in places with the cross stratification typical of low-sinuosity channels, laterally and vertically related to open-lake bioclastic limestone facies. Ubiquitous vertical sequences represent the passage from oncoid-bearing channels to shallow lacustrine and palustrine environments (Arenas et al., 2000). The
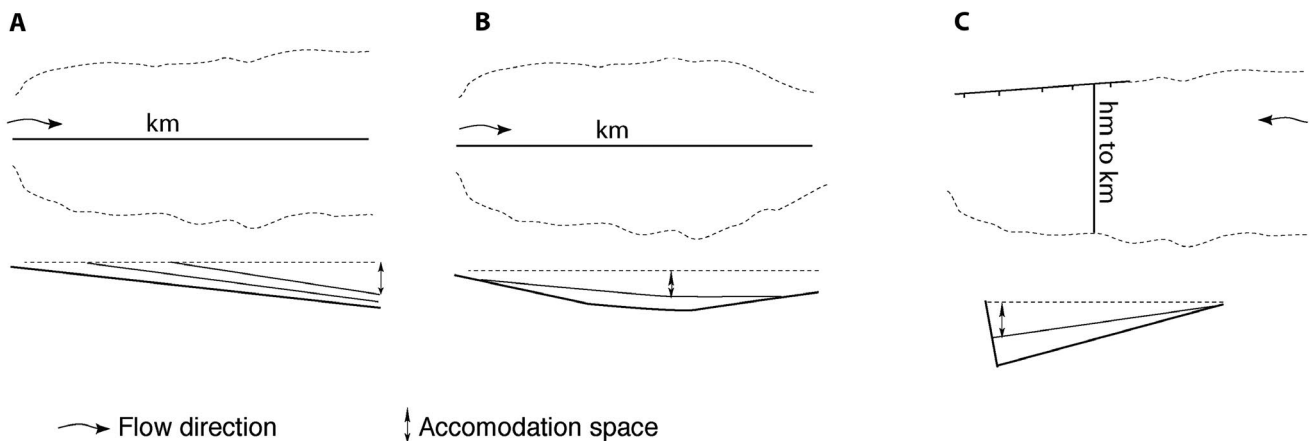
FIGURE 8 Examples of development of fluvial and fluvial–lacustrine environments in plan view and cross-sections. (A) Low-angle wedge-shaped and lenticular bodies along flow. (B) Lenticular bodies along flow. (C) Wedge-shaped bodies across flow. B and C correspond to more subsiding areas due to substrate dissolution (B) and fault activity (C)
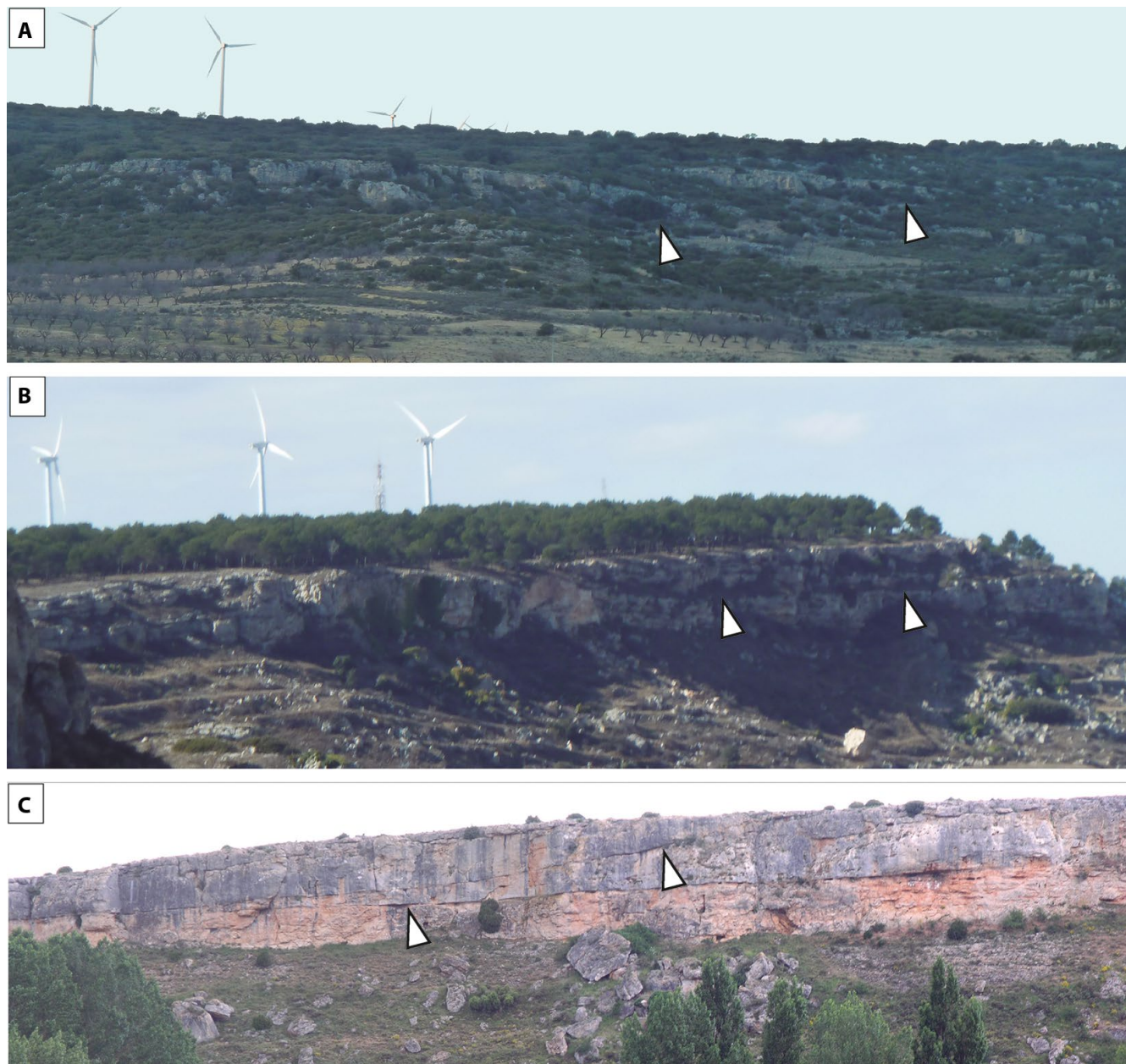
FIGURE 9 Field views of lenticular (A and B) and wedge-shaped (C) bodies (arrowed) forming in low-gradient fluvial and fluvial–lacustrine systems. Dominant facies are oncoids and calcite-coated stem rudstones and boundstones. (A and B) Borja, Ebro Basin, upper Miocene. (C) Añamaza, Iberian Range close to the Ebro Basin, upper Miocene

age of these deposits is probably upper Miocene and it has been proposed that these could represent the downstream portion of the depositional system at Borja (Vázquez-Urbez et al., 2013).

The Upper Jurassic carbonates in the La Vega Formation (Asturias, northern Spain) are dominated by oncoid and phytoclast rudstones, centimetres to decimetres in diameter, forming decimetre-thick deposits, and less common bioclastic limestones. These carbonate deposits are interbedded within a siliciclastic fluvial unit and represent another example of sediments interpreted as having formed in low-gradient conditions, in this case in a rift basin (Arenas et al., 2015b). As

with the Miocene examples, rapid changes of facies and rarity of stromatolites characterised this system. The Oligocene fluvial–lacustrine system in Mallorca is an example of foreland conditions, where the oncoids can reach a few metres in length (Arenas et al., 2007). Despite these two examples fitting the low-gradient model, the outcrop continuity is limited, thus precluding conclusions regarding the geometry of the sedimentary bodies or units. In all these low-gradient systems, oncoids and phytoclasts were dominant in the channel fill, and up-growing hydrophilous plants occupied extensive areas in the channel banks, pool margins and interchannel zones.
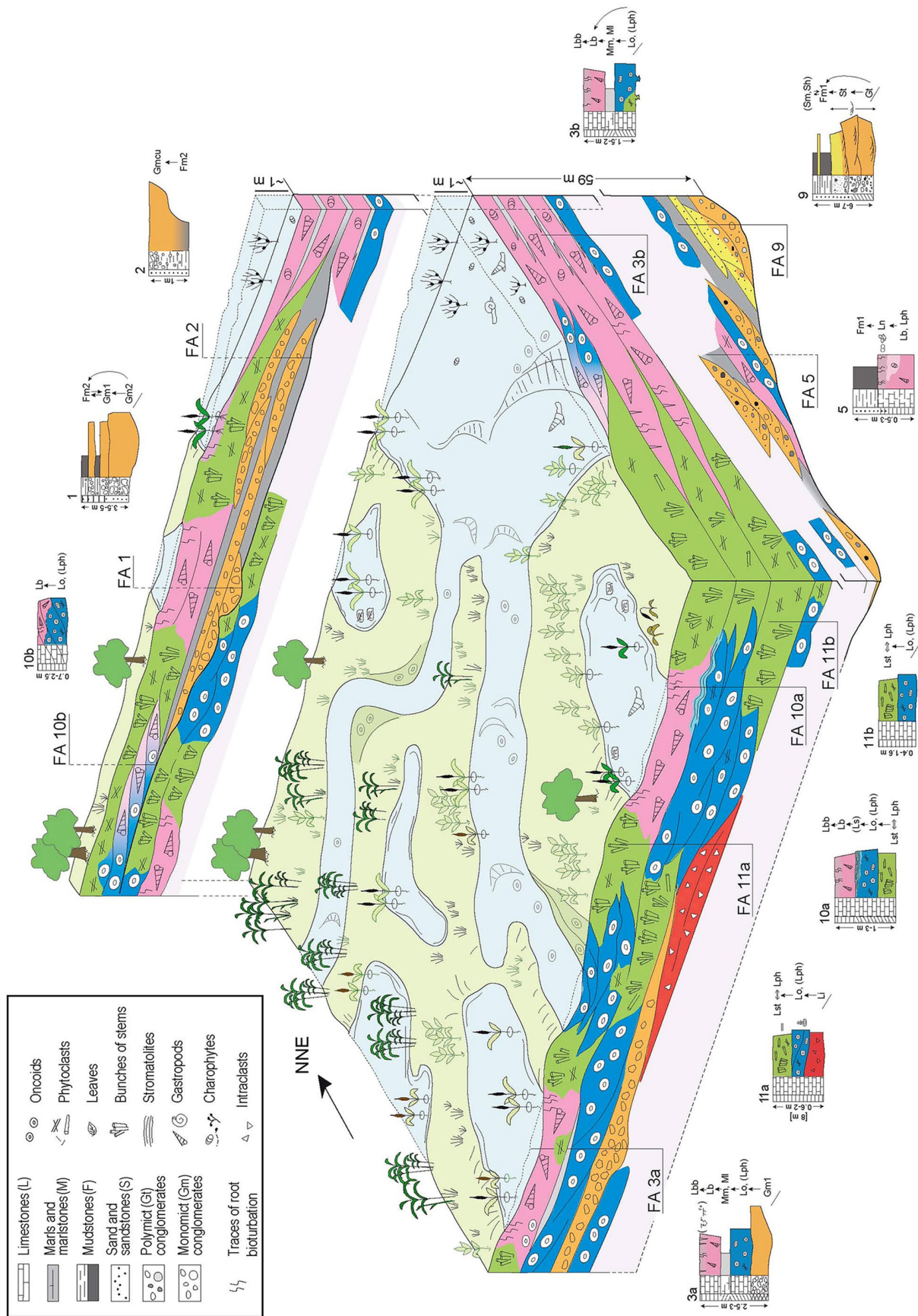
FIGURE 10 Sedimentation model proposed for the low-gradient, non-stepped, fluvial, palustrine and open lacustrine system of the upper Miocene deposits of unit T8 in Borja, indicating common FA. Note abundant oncoids (Lo) and stem limestones (Lst, Lph) and rare stromatolites (Ls). Adapted from Vázquez-Urbez et al. (2013), reproduced with permission of SEPM

2.2.2 | Structure, texture and stable isotopes

The most abundant laminated microbial structures in fluvial low-gradient conditions are oncoids and plant coatings (i.e. from stem rudstones and up-growing stem boundstones). The size and shape of these elements greatly depend on the shape of the nuclei and on the hydrodynamics (Figure 11B) (Arenas et al., 2003, 2007; Astibia et al., 2012; Verrecchia et al., 1997). Commonly the laminae have varied thicknesses, continuity and shape, with the undulate laminae being most abundant (Arenas et al., 2000, 2007; Hägele et al., 2006; Talanda et al., 2017; Zamarreño et al., 1997). Typically, these laminated deposits show conspicuous evidence of microbial activity, through the presence of shrub-shaped, fan-shaped and tabular structures formed of radially arranged and straight bodies, which resemble the shape of the organism, but also through varied lamina shapes and lamination styles. These former features fit well with the skeletal stromatolites (Figure 11C,D,F) (cf., Riding, 2011).

An example of the upper Miocene lamination in Borja
In the oncoids and phytoclasts (stem coatings) of unit T8 in the area of Borja, the laminae are festooned and wavy and rarely smooth, with high lamina-shape inheritance and a variable degree of continuity (Figure 11C). There are, again, two typical types of alternating laminae: (a) dense, dark laminae consisting of micrite, and (b) porous, light laminae consisting of micrite and microspar, commonly with abundant cyanobacterial evidence, with gradual upward transitions from the porous to the dense laminae (Figure 11C). The thickness of the laminae is very variable. Most laminae are composite, that is, they consist of a dominant textural type intercalated with thinner lamina of the other textural type/s (Figure 11C). Both textural types of laminae contain abundant cyanobacterial filaments forming adjacent fan-shaped and shrub-shaped bodies, which are responsible for the undulate shape of the laminae in cross-section (Figure 11D).

The stable isotope composition of oncoids and phytoclasts is typical of meteoric waters, with mean values of $\delta^{13}C = -8.07 \pm 0.53$ and $\delta^{18}O = -6.56 \pm 0.74\%o$ VPDB; $N = 15$. The values are typical of fresh water. The poor correlation coefficient between C and O suggests open lacustrine conditions (Vázquez-Urbez et al., 2013). Differences between the dense and porous laminae have not been analysed yet.

Other examples
In the Upper Jurassic La Vega Formation, the oncoid laminae are also festooned and wavy and rarely smooth, with high lamina-shape inheritance and a variable degree of continuity (Figure 11E,F). Calcitic oncoids show a cyclic variation in both $\delta^{13}C$ and $\delta^{18}O$ values, with the dense/dark laminae having less negative values and the porous/light laminae

more negative values. Despite the differences being small (Table 1), these changes suggest seasonal to multi-annual variations in precipitation and temperature, which impacted the textural features of the laminae (Arenas et al., 2015b).

A classic work is that of Zamarreño et al. (1997), which found small isotopic differences between the light and dark laminae of oncoids formed in the Eocene fluvial deposits of the Eastern Ebro Basin (Figure 2 for location). No significant difference was observed in the isotopic composition of thick light and thin dark laminae in these deposits, suggesting no relationship between the isotopic composition and the textural variations. The authors suggested as a plausible explanation the lack of seasonal contrast either in water $\delta^{18}O$ values or in temperature between the rainy and dry seasons that characterised their formation in a tropical climate zone.

2.3 | Low-gradient closed lacustrine systems

2.3.1 | Depositional geometry, architecture and facies models

Carbonate-depositing lakes with laminated microbialites are ubiquitous through time (Gierlowski-Kordesch, 2010; Kelts & Talbot, 1990, and references therein). Stromatolites and oncolites in lakes occur in diverse environmental and hydrological conditions, including variations in factors such as water depth and salinity, hydrodynamics and the slope of the lake floor (Della Porta, 2015; Harris et al., 2013; Platt & Wright, 1991). Platt and Wright (1991) proposed a classification of lakes based on energy and slope, in which all possible combinations could be favourable for microbialite formation. However, although examples of modern and ancient microbialite-bearing lakes can fit that classification, there is not a clear/direct consideration of the geometric characteristics of the microbialite-bearing sedimentary units that fill the basins. It is therefore difficult to propose geometrical variations of microbialite-bearing bodies based on those examples. Except for a few works (Deschamps et al., 2020; Roche et al., 2018), there are few examples that integrate the geometry of the microbialites or the microbialite-bearing units in the context of a sedimentary facies model, or relative to the units that fill the basin. These examples mostly fit the low to high-gradient profile, without the development of a bench (Figure 12). Researching relevant examples in this respect has yielded no applicable results, despite lacustrine microbialites being in vogue with regards to oil exploration over the past few decades (Della Porta, 2015; Harris et al., 2013).

An example of the early and middle Miocene in the Ebro Basin
The Ebro Basin during the latest Oligocene to middle Miocene was a place where large and shallow lakes developed (Muñoz
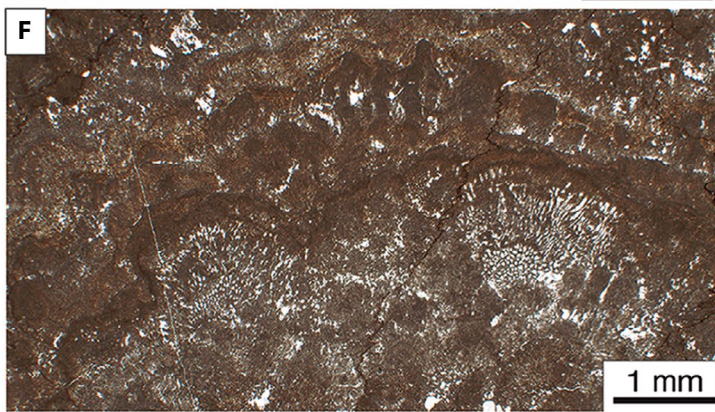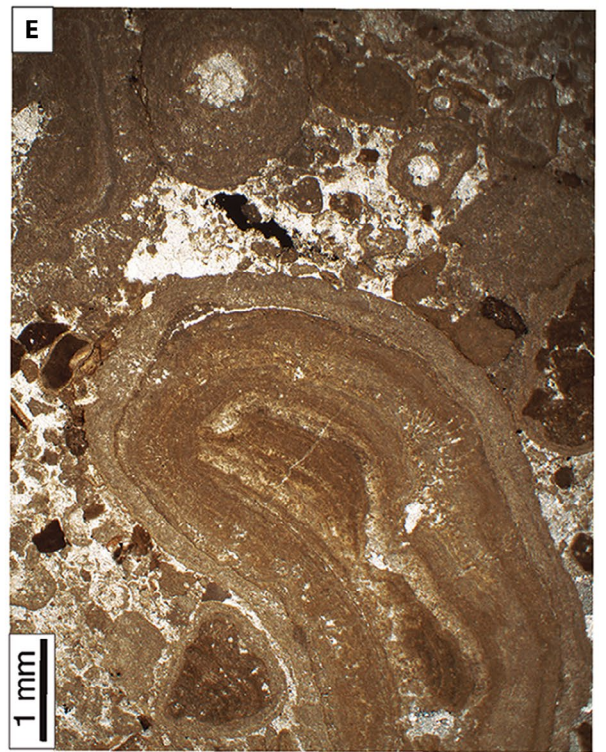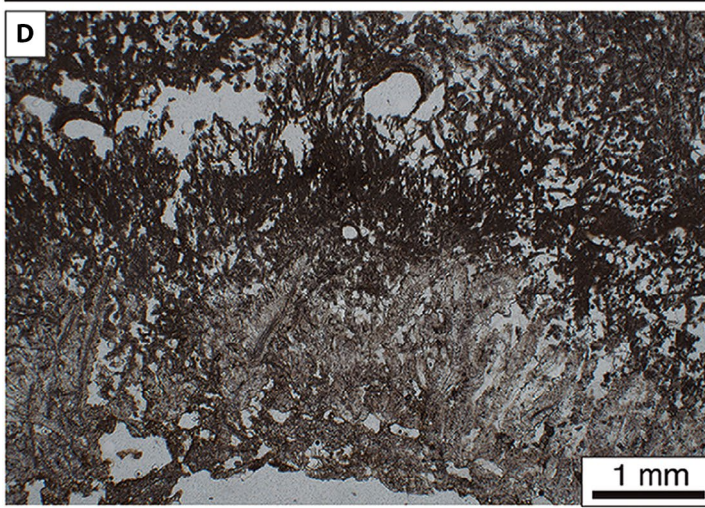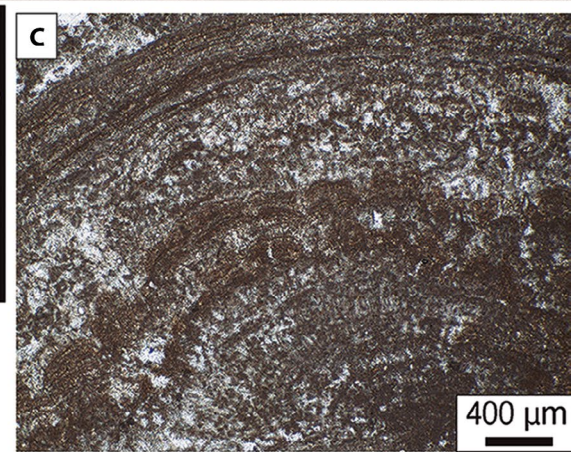
FIGURE 11 Field views (A and B) and photomicrographs (C–F) of oncoids and calcite-coated stem deposits formed in low-gradient fluvial and fluvial–lacustrine environments. (A–D) Borja, genetic stratigraphic unit T8. (A) Gently sloping lenticular deposit formed of oncoid rudstone. Note crude cross stratification and fining upward from base to top. (B) Cross-sections of oncoids showing slightly undulated laminae and varied thickness. (C and D) Lamination consisting of alternating micrite (dark) and microspar (light) composite laminae. Note wavy laminae in half lower half of C. Note in D a palisade of filamentous bodies at the base of a stem coated with calcite. Note larger crystal size coating the filaments at the base passing to micrite upwards. (E and F) Upper Jurassic, Asturias. (E) oncoid rudstone including intraclasts. (F) Wavy lamination resulting from adjacent and stacked fan-shaped bodies consisting of radially arranged filamentous bodies

et al., 2002). Although there are many other examples of ancient lakes in which stromatolites and oncolites may have formed under conditions of different salinity, energy, depth or slope, the Ebro Basin allows for a multi-scale approach. Over that time interval there has been intense research of the central part of the basin (Sierra de Alcubierre and Montes de Castejón; Figure 2) focussing on stratigraphy, sedimentology, geochemistry and magnetostratigraphy, allowing for a robust knowledge of the lacustrine systems and the associated microbialite-bearing units that fill the basin (Arenas et al., 1997; Arenas & Pardo, 1999; Martín-Bello et al., 2019a, 2019b; Pérez-Rivarés, 2016; Pérez-Rivarés et al., 2018, 2019).

From the late Eocene, the Ebro Basin lost its connection with the ocean. The lakes, in the basin centre, received fluvial inputs from the mountain ranges in the north, south and south-east. The lacustrine record of the Burdigalian to Langhian (i.e. genetic stratigraphic units T5 and T6; Pardo et al., 2004) in the central part of the basin, an approximately 500 m thick succession, shows great variability of facies (carbonate, sulphate, halite and siliciclastics). While

Low to high gradient lake

FIGURE 12 Examples of gently sloping lenticular and ramp-shaped bodies developing in low to high-gradient lake margins (without benches). (A) Low gradient. (B) Moderate gradient. (C) High gradient. Microbialites develop extensively along the middle portion in each case. Length is hectometre to kilometre

stromatolites are abundant throughout the sections, oncolites are only found locally.

At macroscopic scale, the stromatolites occur as stratiform bodies up to 40 cm thick and a kilometre in extent, bioherms up to 30 cm thick, and thin, up to 10 cm thick, tabular to lenticular bodies extend for up to a metre (Arenas et al., 1993; Martin-Bello et al., 2019a) (Figure 13). These stromatolites always occur associated with laminated limestones and dolostones, which formed in shallow water subject to both fair-weather and storm conditions (Figure 14). Within the vertical associations of facies, stromatolites occur at the base of deepening cycles (Figure 14D,E) and through shallowing cycles (Figure 14F,G), representing either the beginning of deposition after desiccation and/or erosional processes, or the end of deposition in shallowing-upward sequences (Figure 14G). In detail, stromatolites can be the first deposits after subaerial exposure (Figure 13C) and also after erosion, either in subaerial or subaqueous conditions, in the latter case alternating with laminated limestones in deepening-upward cycles (Figure 15A). Stromatolites through shallowing-upward cycles can be associated, for instance, with laminated limestones with hummocky cross stratification and with microcrystalline nodular gypsum (Figure 13B,D).

These stromatolites and laminated limestones (in places, dolostones) represent carbonate deposition under saline conditions based on their stable isotope composition, the associated facies indicative of salinity and their position in the lake with respect to freshwater facies. Both carbonate facies have less negative $\delta^{13}C$ and $\delta^{18}O$ values than the bioclastic limestone facies. This isotopic difference indicates that stromatolites and laminated carbonate facies formed in water subject to high evaporation which was not frequently renewed (i.e. water with long residence time), thus reaching high salinities compared to the other carbonate facies (Arenas et al., 1997). The sedimentological and geochemical data, along with the spatial distribution of lithofacies, suggests a sedimentary facies model for this carbonate lacustrine system in which the laminated limestones and stromatolites represent inner fringes in the lacustrine system, while the bioclastic, either massive or bioturbated, limestones occupy the outer fringes (Figure 14A). In other words, the stromatolites and laminated limestones represent low lake levels relative to the freshwater carbonate-depositing stages. Thin stromatolites developed in shallow areas and thicker bodies in deeper areas. Storm
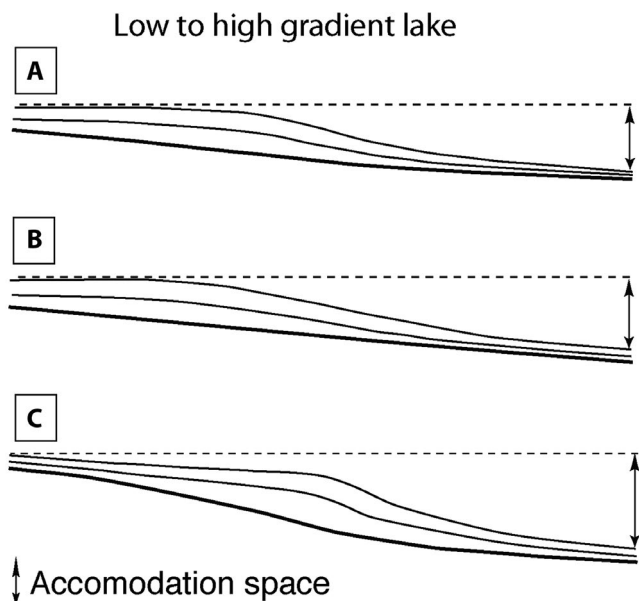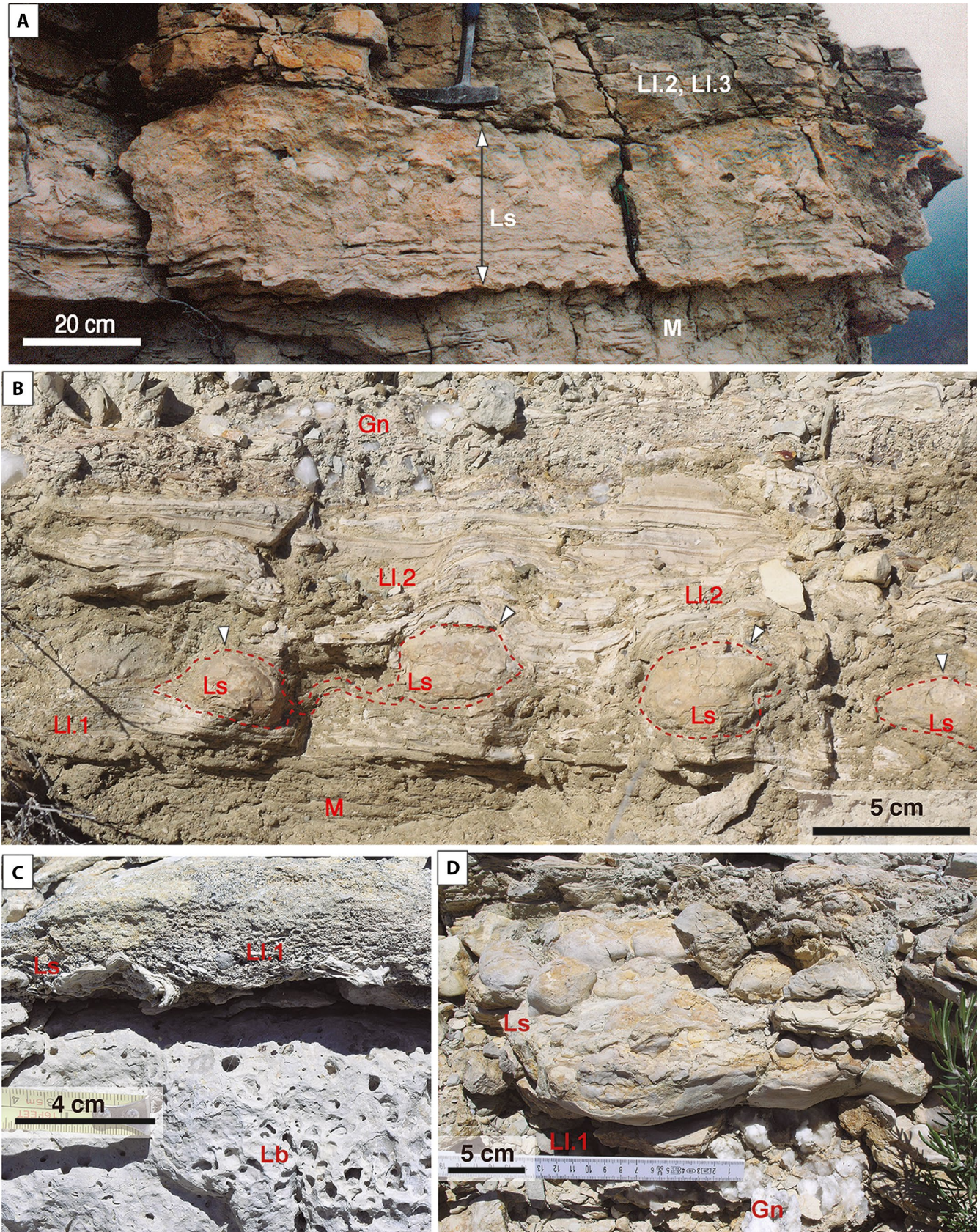
FIGURE 13　Field views of stromatolites (Ls) formed in low-gradient saline carbonate lake, early and middle Miocene in the Ebro Basin. (A) Portion of a stratiform stromatolite. Note lower part with festoons. (B) Small domes (bioherms) associated with ripple and hummocky cross stratification (facies Ll.1 and Ll.2). Note gypsum nodules in the upper part (Gn). (C) Stromatolite thin layer and fragments on a subaerially exposed deposit (Lb), as represented at the base of sequence D of Figure 14. (D) Thin stromatolite with numerous heads at the top of a shallowing sequence, as in sequence G of Figure 14. Legend of facies nomenclature in Figure 14
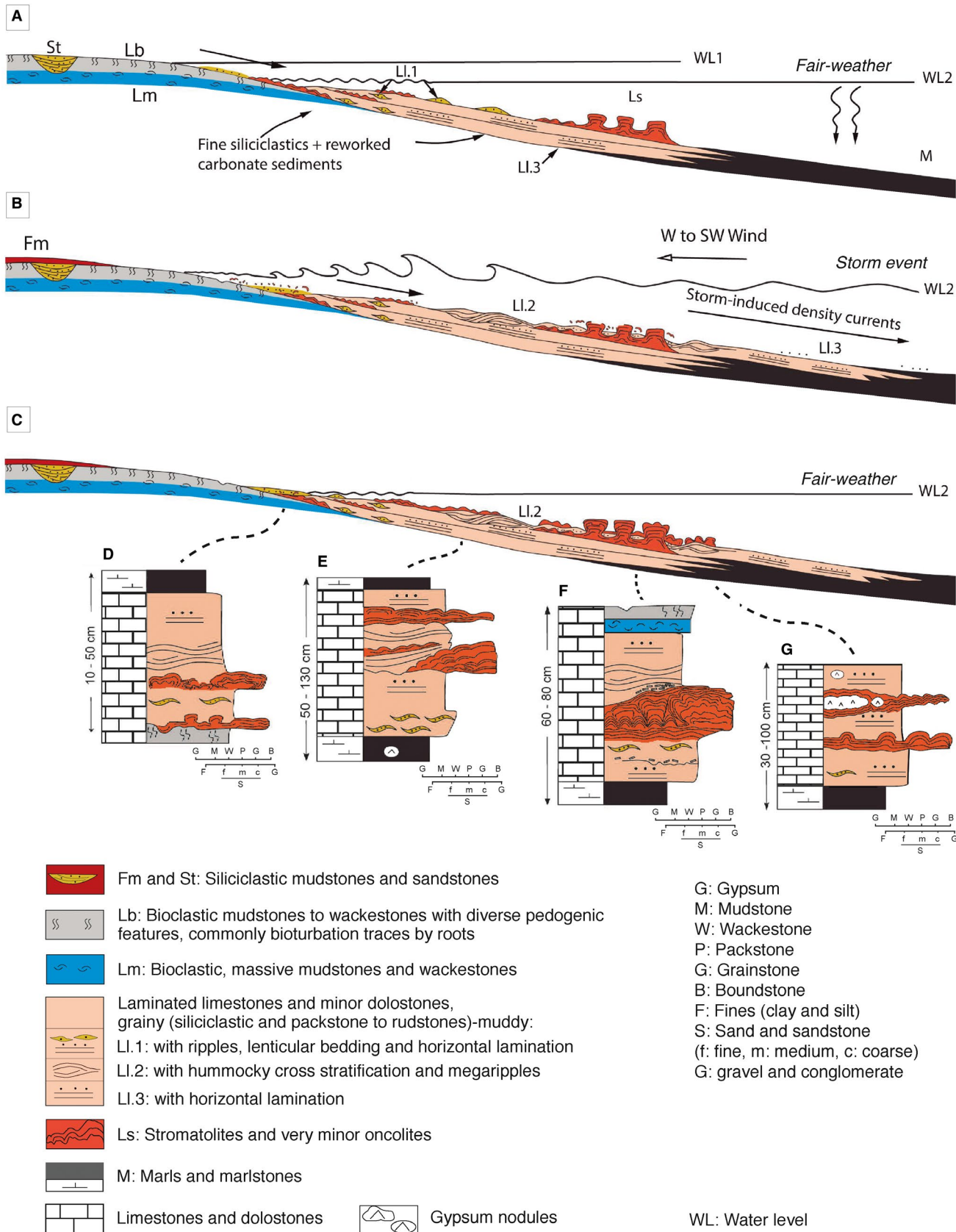
FIGURE 14 Sedimentary model in a low-gradient saline carbonate lake affected by surge processes. Morphologically diverse stromatolites form during low lake-level and fair-weather conditions (A and C). Storm and inflow processes erode coastal deposits, cause surge structures and induce density currents, yielding to the formation of diverse laminated limestones (B). Sequences D–G result from successive lake-level variations. Sequences D and E correspond to a general deepening trend, and sequences F and G to a general shallowing trend. Modified from Martín-Bello et al. (2019a)
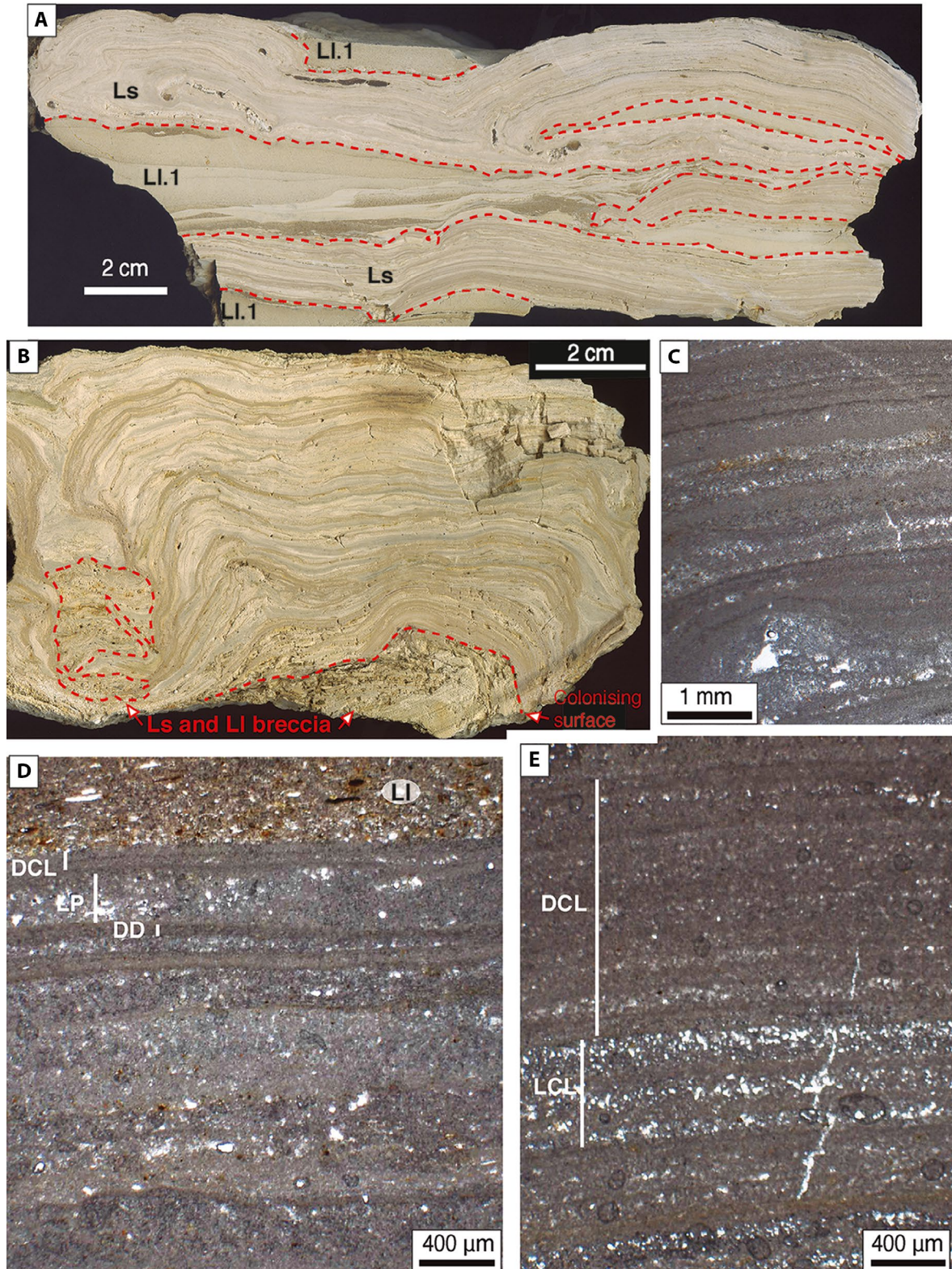
FIGURE 15 Stromatolite lamination in hand samples (A and B) and microphotographs. (A) Intricate relationship between stromatolite (Ls) and laminated limestones (Ll.1). Note erosional surfaces on stromatolites. Sierra de Alcubierre, unit T6. (B) Continuous domed growth form with high synoptic relief of the laminae. Note to the left the interdome area occupied by stromatolite and laminated limestone fragments. Sierra de Alcubierre, unit T5. (C–E) Lamination consisting of alternating dark dense (DD) and light porous (LP) single laminae, and dark composite (DCL) and light composite laminae (LCL). Note grainy sediment (facies Ll) on the top of stromatolite in (D). Note in (C) the domed shape at the base, probably reflecting growth of a microbial body

processes caused erosion of stromatolites, formation of hummocky cross stratification and parallel lamination from density currents (Figure 14B). Much lower lake levels would produce sulphate and halite deposition (Arenas & Pardo, 1999), not represented in Figure 14.

The geometry of the sedimentary units formed of stromatolites and laminated carbonate facies correspond to gently sloping lenses and/or ramp-shaped bodies, decimetres to a few metres thick and a few kilometres long along the lake margin (Figure 14C). This geometry suits a low-gradient lake system (mean gradient of the lacustrine system was estimated to be approximately 0.01°; Arenas & Pardo, 1999). Focussing on the Sierra de Alcubierre and Montes de Castejón, the early and middle Miocene lakes experienced water level changes between the freshwater setting and the saline carbonate setting that involved 5–15 km long migrations of the lake shore.

2.3.2 | Structure, texture and stable isotopes

Most studied microbialite deposits formed in closed lake systems correspond to micritic stromatolites (sensu, Riding, 2000). There are few cases that describe agglutinated stromatolites in saline lacustrine environments, for example, in the Miocene Wudaoliang Group, northern Tibetan Plateau (Zeng et al., 2019) and in the Lower Cretaceous, lacustrine-coastal environment of the Cameros Basin, Spain (Suárez-González et al., 2014). The examples considered here refer mainly to micritic microbialites.

Lamination in the studied Miocene stromatolites of the Ebro Basin is conspicuous, consisting of alternating light and dark laminae, mostly consisting of calcite and in a few cases of dolomite. The laminae are smooth in cross-sections, at mesoscopic and microscopic scale (Figure 15). Light and/or porous micrite and microspar laminae are 0.035–2 mm thick, and dark and/or dense micrite laminae 0.045–2.5 mm thick. Most laminae are composite, that is, formed of a dominant textural type and including thin intercalations of other textural types (Figure 15D,E). Several styles of lamination have been described (Martin-Bello et al., 2019a). Overall, microbial filaments in the studied samples are rarely found. In places micrite filamentous bodies occur perpendicular to lamination; in other cases, the laminae are slightly undulate and/or form domed bodies up to 2.5 mm thick that resemble cyanobacterial growths (Figure 15C).

The stable isotope analyses of the laminae show cyclic variations through time that are parallel to textural changes (e.g. Figure 16 shows high-resolution variations). The cyclic pattern is seen in both $\delta^{13}C$ and $\delta^{18}O$ values through many analysed specimens: dark laminae having less negative values and light laminae having more negative values, with a good correlation between C and O, $r = 0.63$ in unit T5 ($N = 79$), $r = 0.63$ in unit T6 ($N = 80$) and $r = 0.9$ in unit T7 ($N = 15$). The difference between the values of light and dark laminae is 0.38, 0.23 and 0.60‰ for $\delta^{18}O$, and 0.2, 0.16 and 0.17‰ for $\delta^{13}C$, respectively for units T5, T6 and T7 (Table 1).

These cyclic isotopic changes occur at different scales of lamination. There are three orders or ranks of isotopic variations, in which the light laminae are more negative and the dark laminae are less negative. The third-order rank is a simple light and dark couplet, each composite lamina is a second-order rank, and each couplet formed of a composite light lamina and a composite dark lamina represents the first-order rank (Figure 16). The three ranks of isotopic patterns are consistent with textural changes and have been interpreted as representing seasonal to multi-annual variations in the Precipitation/Evaporation rate (P/E; Martin-Bello et al., 2019b).
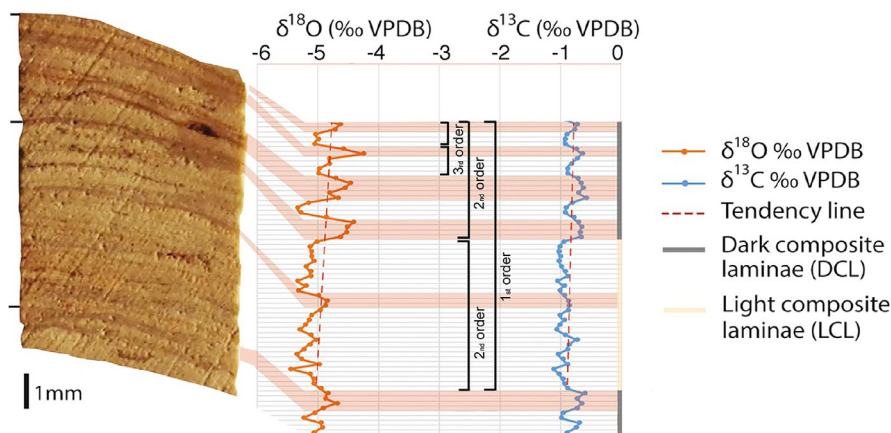
FIGURE 16 Stable isotope evolution ($\delta^{13}C$ and $\delta^{18}O$ values) from high-resolution sampling of a portion of a columnar stromatolite from genetic stratigraphic unit T5 in Sierra de Alcubierre. Note the significant correlation between the less negative values of C and O in the dark laminae and more negative values in the light laminae (for the first order cycle, $r = 0.82$; $N = 57$). Several orders of isotopic cyclicity are indicated, which coincide with lamina ranges based on textural variations. The first order cycle corresponds to two successive composite laminae. Modified from Martín-Bello et al. (2019b)

2.3.3 | Periodicity analysis of lamination

Periodicity analysis of lamination is a tool that may help discern the environmental and climate significance of lamination and the duration of the laminae. This type of analysis, based on lamina thickness and luminance, has been applied to several specimens of stromatolites from the Ebro Basin to estimate the relationship between the periodicity and natural phenomena occurring over calendar or solar-frequency intervals (Pérez-Rivarés et al., 2019). The results obtained from five early and middle Miocene stromatolites of the Ebro Basin reveal significant periods in the power spectrum at around 2.5, 3.7, 5, 7, 10 and 22 (Figure 17). Assuming each light and dark simple lamina couplet corresponds to a year, these periods could be correlated with the typical oscillation bands of different climate-related agents, such as the QBO (Quasi Biennial Oscillation), the ENSO (El Niño Southern Oscillation), the NAO (North Atlantic Oscillation) and sunspots (Pérez-Rivarés et al., 2019).

3 | DISCUSSION

The factors that control the diverse attributes of microbialites and the evolution of the microbialite-bearing systems are multiple and can produce different effects depending on the scales of study.
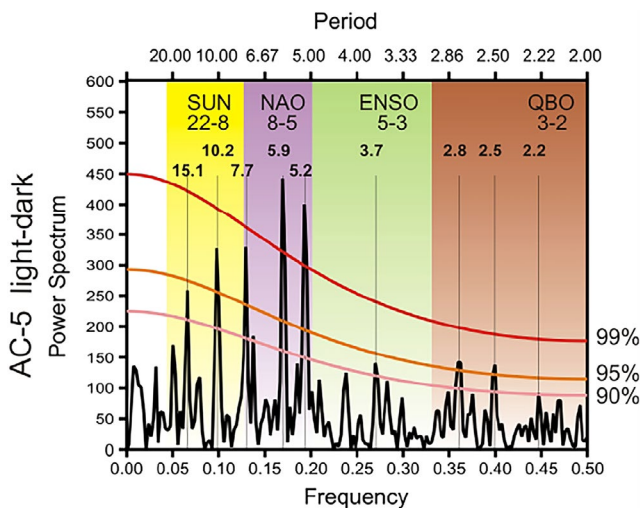
FIGURE 17 Example of periods obtained from periodicity analysis based on lamina thickness (dark plus light lamina thickness) in a stromatolite of genetic stratigraphic unit T5 in the Sierra de Alcubierre (sample AC-5). Probable calendar and solar band frequency cycles are indicated. Note highly significant periods coinciding with NAO frequency. From Pérez-Rivarés et al. (2019), reproduced with permission of Elsevier
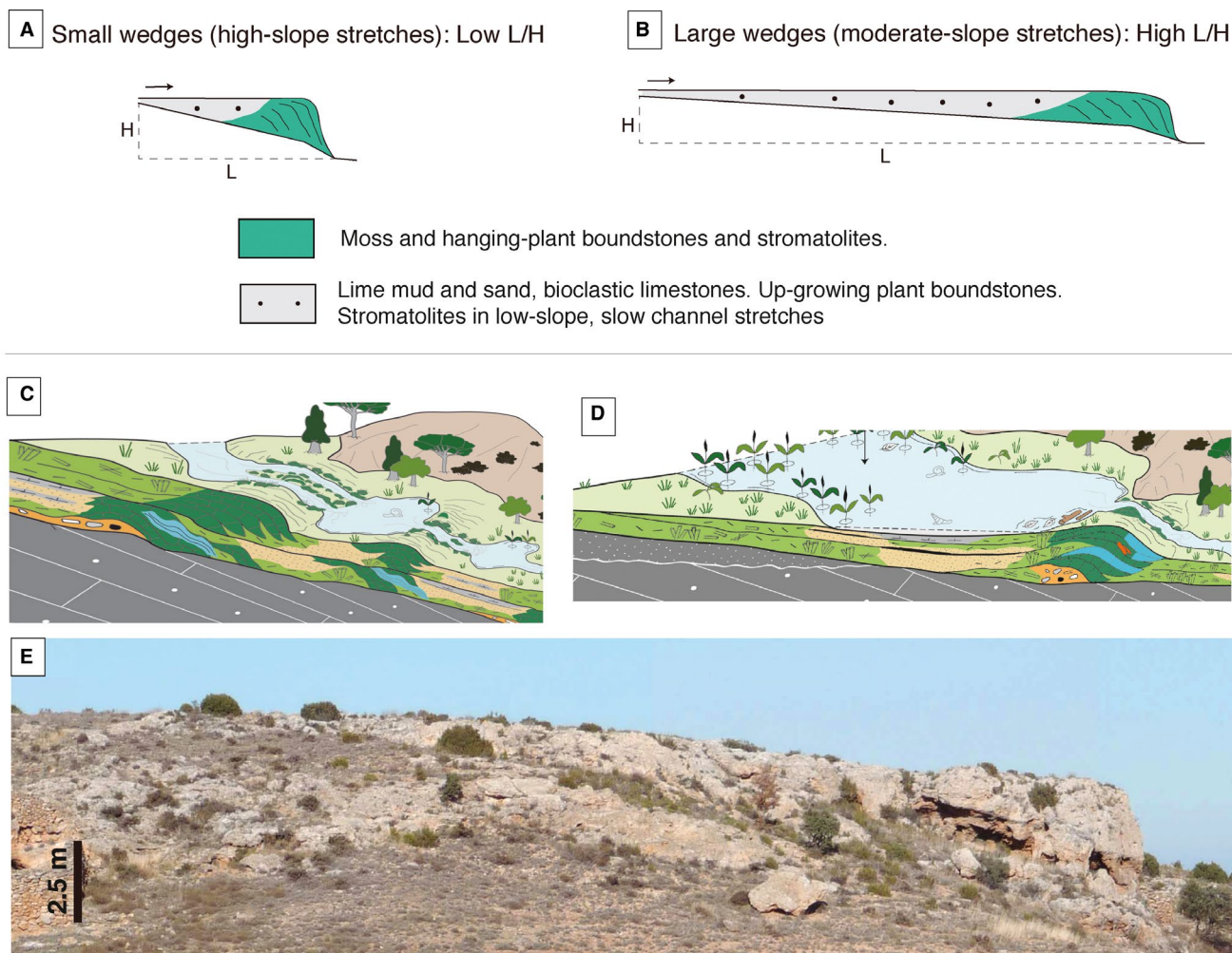
3.1 | Megascopic and macroscopic characteristics: A variegated record of extrinsic and intrinsic factors

The examples considered in this work show clear differences in the geometry of the laminated microbialite bodies and/or the lithosomes with which the microbialites are associated, that is the distinct 3D-geometry and dimensions within the sedimentary units. Indeed, the different positions of the microbialites in the vertical associations of facies have particular environmental significance. The factors that control these features are thus expected to be different and/or produce different effects at different scales. The geometry of the microbialite deposits in the basin sedimentary fill varies as a function of the floor topography, hydrology and occurrence of erosional processes, apart from autocyclic depositional processes. Subsidence and tectonics can also control the geometry and thickness of the sedimentary units (Arenas et al., 2000; Della Porta, 2015; Roche et al., 2018). Figures 18–20, and Table 2 illustrates some of the megascopic and macroscopic features encountered.

In the lenticular and wedge-shaped units that characterise the moderate-gradient and high-gradient fluvial carbonate systems, the dominant laminated microbial structures are stromatolites, which form primarily at the stepped cascades, cascade-barrages and rapids, and calcite-coated stems, either rudstones or boundstones, which are ubiquitous (Figure 18).

The initial knickpoint geometry (e.g. due to changes in the bedrock lithology) and variations in the aggradation/progradation ratio at each knickpoint control the geometry of the depositional units that fill the fluvial valleys, in particular the length/height relationships, that is, L/H (Arenas et al., 2014a; Arenas-Abad et al., 2010). Hydrological conditions (i.e. water discharge) are directly involved in the progradation versus aggradation processes that cause different waterfall styles in front of or at the knickpoints (Arenas et al., 2014b).

The typical half dome and lenticular geometry of the stromatolite bodies respond to the topography of the depositional surface, which tends to favour rapid deposition in areas of moderate to high water flow. Thus, ongoing deposition favoured by rapid flow conditions contributes to the shape of the deposit by exaggerating the initial shape (Arenas-Abad et al., 2010; Pedley, 1990; Pentecost, 2005; Vázquez-Urbez et al., 2012; Violante et al., 1994). The characteristics of present-day, fluvial carbonate systems support the above geometric and depositional evolution (Arenas et al., 2014a; Ordóñez et al., 2005; Pedley, 2009). The fact that these bodies develop along slopes indicates that microbial mats prefer to grow under moderate to rapid flow conditions Modern fluvial tufa systems with microbial mats have shown the highest depositional rates in the fastest flowing areas, with values ranging from 0.6 to 1.7 cm/year (Arenas et al., 2014a; Drysdale & Gillieson, 1997; Gradziński, 2010; Ordóñez et al., 2005).

A Small wedges (high-slope stretches): Low L/H

B Large wedges (moderate-slope stretches): High L/H

Moss and hanging-plant boundstones and stromatolites.

Lime mud and sand, bioclastic limestones. Up-growing plant boundstones. Stromatolites in low-slope, slow channel stretches
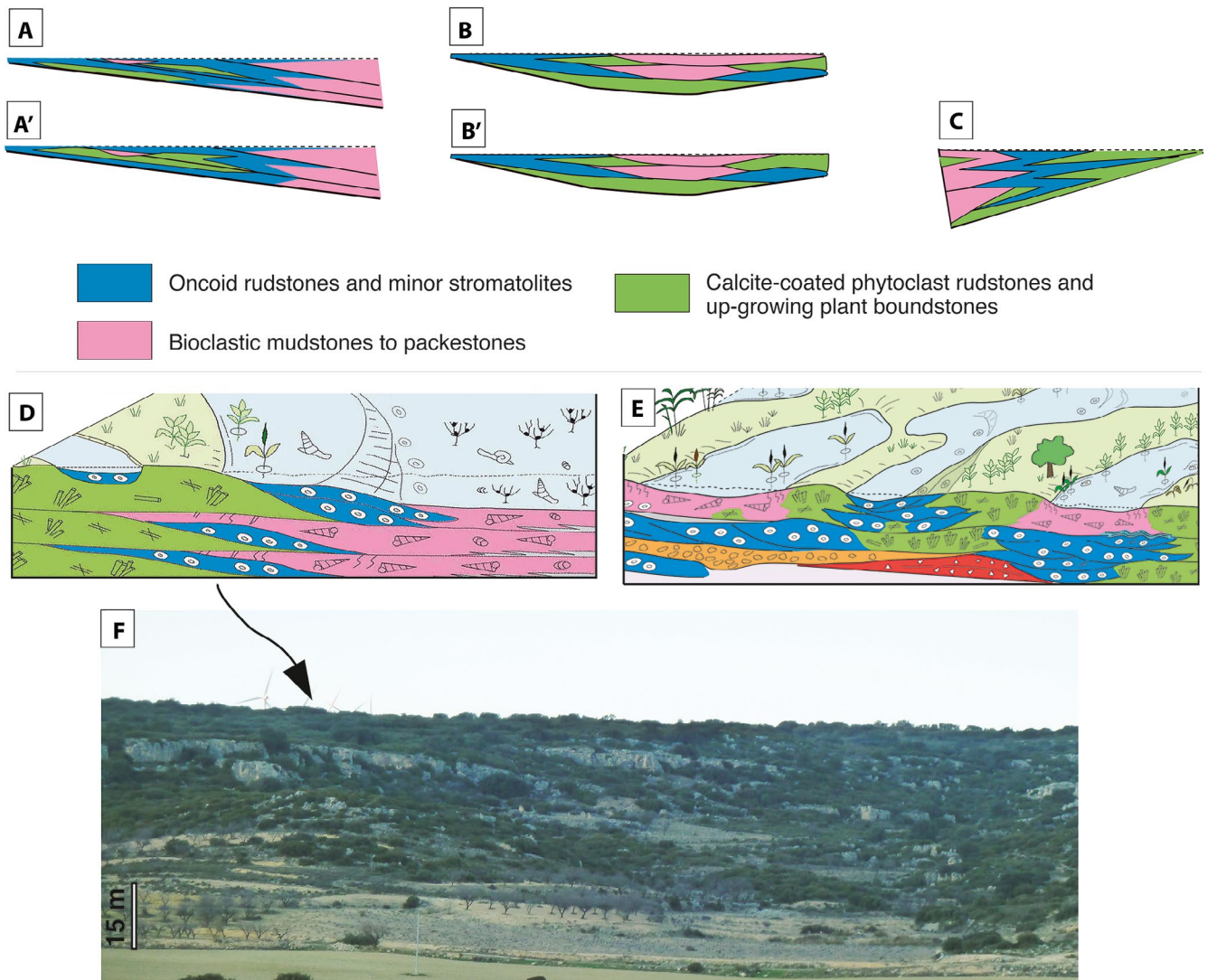
FIGURE 18 Summary of geometric and facies variations in the laminated microbialite-bearing units in (A) high-gradient and (B) moderate-gradient fluvial carbonate systems. (A) Small wedges. (B) Large wedges. (C and D) The depositional situations represented by A and B, respectively. (E) Field image representing an intermediate situation between A and B

In low-gradient, fluvial and fluvial–open lacustrine carbonate systems, without stepped longitudinal profiles, the depositional units, that is, lithofacies, form extensive, low-angle lenticular, ramp-shaped and tabular bodies. The dominant laminated microbial structures are oncolites and calcite-coated stems, either rudstones or boundstones (mainly of up-growing stems). Stromatolites are less common. Most of these systems are characterised by having rapid lateral changes of facies, as shown in Figure 19. Examples that fit this profile have been investigated by Mäcker (1997), Meléndez and Gómez-Fernández (2000), Astibia et al. (2012), Vázquez-Urbez et al. (2013), Arenas et al. (2000, 2007, 2015b) and Talanda et al. (2017).

Thick aggrading units can be preserved in areas subject to high subsidence. For instance, synsedimentary subsidence due to evaporite dissolution caused the thick accumulation of lenticular-shaped carbonate units during the upper Miocene in the Montolar hill area, in the Ebro Basin (Arenas et al., 2000), as shown in Figure 19B. Depending on the structural

control, thickness and facies variations may result in highly asymmetrical basin fills (Meléndez & Gómez-Fernández, 2000; Santos Bueno et al., 2019), as shown in Figure 19C. Lacustrine facies may become dominant downstream and vary in extent depending on climate and/or tectonic conditions (Vázquez-Urbez et al., 2013).

The geometry of the oncoid and calcite-coated stem-bearing bodies (lithosomes) seems to be controlled by intrinsic factors of the depositional settings, ultimately the distribution of the different lithotopes, which can also determine the lateral extent (e.g. such as the channel bedforms; Figure 19D,E). Low-sinuosity channels in wide palustrine zones typically produce the above-mentioned, commonly found geometric types of deposits (Nickel, 1983; Vázquez-Urbez et al., 2013). Nonetheless, high-sinuosity channel styles may produce more markedly lenticular-shaped bodies, as described in the Cenozoic of the Madrid Basin (Ordóñez & García del Cura, 1983), the Ebro Basin (Zamarreño et al., 1997) and the Guadix Basin (García-García et al., 2014).

FIGURE 19 Summary of geometric and facies variations in the laminated microbialite-bearing units in low-gradient fluvial and fluvial–lacustrine carbonate systems. (A and A′) Low-angle wedges and lenses consisting of asymmetric distribution of facies along flow, showing slight differences in facies distribution between A and A′. (B and B′) Lenticular bodies consisting of symmetric distribution of facies along flow, showing slight variation in facies development between B and B′. (C) Wedges consisting of asymmetric distribution of facies across flow, as illustrated in Figure 8C. Increasing subsidence from A to C. (D and E) represent the depositional situations of A and A′. (F) Field image corresponding to D and representing situation A

Extensive, commonly shallow in thickness, gently sloping lenticular and tabular oncoid deposits can also result from channel overflooding onto the alluvial plain, as described in the Oligocene deposits of Mallorca, Spain (Arenas et al., 2007), the Upper Cretaceous of the Tremp Basin, Pyrenees (Astibia et al., 2012 and references therein) and Upper Triassic deposits of southern Poland (Talanda et al., 2017).

The deposits of low-gradient, fluvial and fluvial–open lacustrine carbonate systems are particularly well preserved in rift or semi-graben settings, thus it is suggested that subsidence is a main control on the accumulation and preservation of thick aggrading carbonate deposits (Figure 19B,C). In contrast, these subsiding settings are less common in the case of moderate-gradient and high-gradient carbonate fluvial systems, which may partially explain the rarity of thick tufa sequences in the geological record (Arenas-Abad et al., 2010).

In low-gradient closed lake systems, such as the Miocene saline carbonate record in the Ebro Basin, laminated microbialites form part of extensive gently sloping lenticular and ramp-shaped units, and the dominant facies are stromatolites. The geometry and extent of these units are controlled by the small slope of the lake floor's surface and the shallow water depth, which, based on changes in the FA, varies by up to 4 m. Within these units, the stromatolites constitute extensive tabular bodies, small bioherms and very abundant thin bodies that are associated with grainy-muddy laminated facies (Figure 20). The geometry of these microbial structures seems to be related to
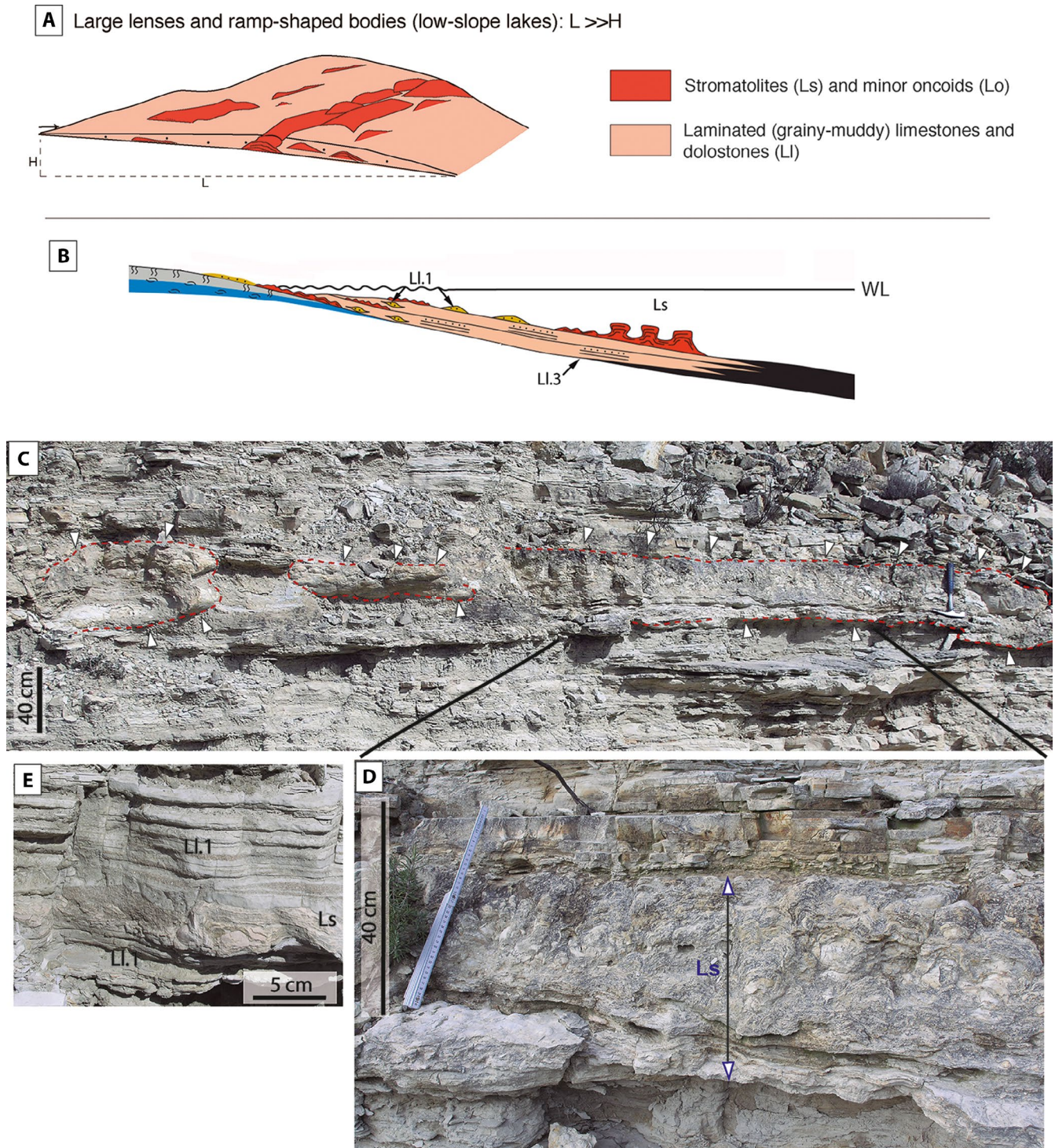
FIGURE 20 Summary of geometric and facies variations in the laminated microbialite-bearing units in low-gradient lacustrine carbonate systems. (A) Sketch representing the large lenses and ramp-shaped bodies, showing the position of microbialites. (B) Distribution of microbialite-bearing lenses and ramp-shaped bodies in the sedimentary facies model for the early and middle Miocene in the Ebro Basin. (C, D and E) Field images showing the range in stromatolite morphology (arrows in C) and their associated facies (Ll). Facies codes in Figure 14

the water level and hydrodynamic conditions in this part of the basin (Casanova, 1994; Martin-Bello et al., 2019a), rather than to tectonics or subsidence. Lacustrine stromatolites associated with surge activity as seen in the Ebro Basin have not been extensively reported in other basins, except for a few reports from the late Archean in Western Australia (Awramik & Buchheim, 2009), in the Eocene of Green River Formation (Graf et al., 2015), and in the Oligocene–Miocene lacustrine microbial and metazoan buildups in the Limagne Basin, French Central Massif (Roche et al., 2018).

TABLE 2 Summary of principal low-frequency and high-frequency features from several examples mentioned in the text. (a) Arenas et al. (2014a, 2015a), Osácar et al. (2016; Osácar Soriano et al., 2017), Arenas and Jones (2017). (b) Vázquez-Urbez et al. (2012), Arenas et al. (2014b). (c) Vázquez-Urbez et al. (2013), Arenas et al. (2015b). (e) Martín-Bello et al. (2019a, 2019b). (f) Roche et al. (2018)

Environments	Fluvial carbonate systems — High gradient and moderate gradient	Fluvial and fluvio-(open) lacustrine carbonate systems — Low gradient	Lacustrine carbonate systems — Low slope	High slope
Examples described or cited in text; Geodynamic context/Hydrology	Recent rivers, Iberian Range (a) Quaternary, Iberian Range (b); Stable/Free flowing fresh water	Cenozoic, Ebro and Balearic basins (c) Late Jurassic, Asturias (d); Foreland/freshwater	Lower-middle Miocene, Ebro Basin (e); Foreland/closed saline lake	Lower Miocene, Limagne Basin (f); Half graben/freshwater
Dominant laminated microbialites	Stromatolites and calcite-coated stems, rare oncoids	Oncoids and calcite-coated stems, rare stromatolites	Stromatolites, rare oncoids	
Mega and macroscopic features				
Geometry of microbialite-bearing units	Large and small wedges and lenses	Lenses, low-angle wedges and tabular bodies	Large lenses and ramp-shaped bodies	Larges lenses and conspicuous sigmoidal bodies?
Morphology of microbialites	Domed, half domed, highly inclined lenses and minor tabular	Spherical, ovoid and elongated	Stratiform, domed and thin flat	Coalescent columnar, domed, conical and flat
Internal growth forms	Commonly gentle undulate layers. Rare columns.	Varied: columns, domes and gentle undulate layers	Columns, domes and gentle undulate layers	Columns, domes and gentle undulate layers
Meso and microscopic features				
Lamina shape (outline)	Flat, gentle undulate to festoon, rare smooth	Wavy and festoon, rare smooth. Varied continuity	Common smooth and continuous	Varied; common wavy and festoon laminae
Structure and texture	Composite dense and porous micrite, microspar and spar laminae representing seasonal to six-month periods. Arthropod moulds	Composite dense/dark micritic and porous/light micrite or spar laminae of unknown duration. Arthropod moulds	Dark and light dense micrite, and light porous microspar. Simple laminae couplet yearly. Rare fibrous laminae. Rare microbial evidence	Micritic-dominated and cement-dominate laminae. Arthropod moulds. Common and varied-shaped bacterial bodies
Microbial evidence	Varied. Common cyanobacterial filaments. Diatoms			
Sedimentation rates (mm/year)	4–17[a] 2.5–8.3[b]	—	0.2–0.6[c]	—
Stable isotope composition of the laminae (‰ V-PDB)	Lack of correlation between $\delta^{13}C$ and $\delta^{18}O$ values. Irregular variation of $\delta^{13}C$ values, or locally opposite to that of $\delta^{18}O$. Influence of residence time of water in aquifer. Cyclic pattern of $\delta^{18}O$ values through time accurately reflect water temperature		Strong $\delta^{13}C$ and $\delta^{18}O$ correlation. Seasonal to Pluriannual changes in P/E and biological $^{12/13}C$	—

The geometry of the microbial deposits and the features of the internal growth forms have been used to infer varied environmental and climate characteristics, such as water level, hydrodynamics and sediment supply. There is large consensus on the interpretation of such geometric variations (Bouton et al., 2016; Martín-Bello et al., 2019a; Roche et al., 2018; Tosti & Riding, 2017; Vennin et al., 2019). Also, on a megascopic scale, referred to the vertical sequences of facies, the geometry and distribution of stromatolites and their relationship with other facies are used to indicate water level, hydrodynamics and salinity changes through time (Arenas et al., 1993; Arp et al., 2005; Lettéron et al., 2018; Martín-Bello et al., 2019a; Seard et al., 2013). On longer sequences, the evolution of the geometric characteristics and distribution of the stromatolite bodies through time has been used to support changes in climate that impact the lake water level and the consequent accommodation space, such as in the Limagne Basin (French Central Massif) during the transition from the Oligocene to the Miocene (Roche et al., 2018). There, the change from thin to thicker stromatolites is interpreted as representing a change to warmer and more humid conditions and a higher-slope margin lake during the Aquitanian.

The Bonneville Basin, currently occupied by the Great Salt Lake, records a high lake-level phase (Pleistocene Bonneville lake) and a low lake-level phase (Holocene to present lake) (Bouton et al., 2016; Vennin et al., 2019). In both phases the distribution and geometry of stromatolite-bearing units or the stromatolite bodies reflect the basin floor configuration (extent and slope). The Holocene-to-present phase depicts more extensive units, with varied stromatolite morphology, centimetre to 30 cm thick bodies, as a result of the flat topography and lake-level variations, probably similar to the lower to middle Miocene in the Ebro Basin.

Some stratigraphic units of the Eocene Green River Formation (USA) contain stromatolites formed in shallow saline lakes (Chidsey et al., 2015; Graf et al., 2015; Pietras & Carroll, 2006; Scott & Smith, 2015; Seard et al., 2013; Smith et al., 2015; Smoot, 1983), although the large-scale geometry of the microbialite-bearing units has not been depicted in detail in all cases. In the Tipton and Wilkins Peak Members (Lake Gosiute, Green River Basin), the stromatolites form decimetre-thick and kilometre-long bodies, which are interpreted as having grown in littoral zones of a saline lake with rapid lake-level fluctuations and intense hydrodynamic activity (Graf et al., 2015). The geometry and environmental conditions proposed in this example resemble the Ebro Basin. In the Parachute Creek and Douglas Creek Members, in the Uinta Basin, Chidsey et al. (2015) described domed stromatolites developed on grainy limestones, as seen in the Ebro Basin saline carbonate lakes.

The rarity of oncoid deposits in the saline carbonate lake of the Ebro Basin could be related to difficulties with microbial accretion on moving grains in an environment affected episodically by high energy processes (e.g. storm periods producing erosion and inflows). A similar situation is also seen with other saline lakes (Bouton et al., 2016; Chidsey et al., 2015; Graf et al., 2015). The high energy environment can explain the rarity of oncoids in the moderate-gradient and high-gradient fluvial systems experiencing continuous strong current flow. For example, the asymmetrical oncoids currently forming in the River Alz (south Germany) experience very little movement (Hägele et al., 2006). Therefore, from the studied examples herein, it appears that oncoids are better developed and preserved in low-gradient fluvial and fluvial–lacustrine environments. Nonetheless, the behaviour of fluvial oncoids during transportation and deposition cannot be easily predicted, as was shown by Verrecchia et al. (1997). Some saline and freshwater lakes that are not subject to energetic water flows allow for the formation and preservation of oncoids, such as in the present Laguna Pastos Grandes, in Bolivia (Jones & Renaut, 1994) and Baringo Lake, in Kenya (Renaut et al., 2002). Both lakes receive hydrothermal inflows.

3.2 | Mesoscopic and microscopic characteristics of lamination: An array of low-frequency proxies

The main differences in the lamination of the studied micritic stromatolites concern lamina shape and thickness (Table 2). Lamina shape is diverse, and thickness is high in the fluvial environment, while in the saline lacustrine environment the laminae are smooth and thin and can be isopachous. Other relevant differences concern the varied and well-preserved bacterial evidence (commonly cyanobacterial) in the fluvial and open lacustrine record, while such evidence is rare in the saline lake record.

In low-gradient freshwater fluvial and fluvial–lacustrine systems, the microbialitic lamina shape in oncoids and stem calcite coatings is linked to the morphology of the biological component, thus explaining the festooned and shrubby or wavy shapes of the laminae (Hägele et al., 2006; Arenas et al., 2007). Likewise, freshwater oncoids and stromatolites formed in Miocene lakes of New Zealand showed thick laminae with festooned shapes reflecting the growth form of cyanobacteria and other bacteria (Lindqvist, 1994). In turn, the lamina continuity is a function of hydrodynamics, reflecting the frequency with which the grains overturn and changes in water energy (Arenas et al., 2007, 2015b; Lindqvist, 1994; Zamarreño et al., 1997).

In contrast, in the saline lake environment the laminae tend to be smooth, which can reflect the low relief and/or poor morphological diversity of the microbes. Despite the type of microbes being unknown in the investigated Ebro Basin example—although these probably were coccoid and rare

filamentous bacteria—, it seems that the chemical characteristics of the water, for example, through salinity, can influence the type of microbes and their morphological diversity, thus influencing the lamina shape. Gallois et al. (2018) described crinkled to flat lamination in lacustrine stromatolites formed in brackish water during the Upper Jurassic–Lower Cretaceous (Purbeck Group) in the Wessex Basin (Dorset, UK). While in the marine environment, shallow platform deposits of the Cambrian in China contain oncoids with smooth-outlined laminae (Han et al., 2014).

3.3 | Environmental and climate (including hydrological) significance of lamination

Generally, textural and geochemical changes between laminae are interpreted in terms of variations in parameters such as temperature, evaporation, precipitation and water discharge, the latter either via surface or from the aquifer, and biological activity (Casanova, 1994; Chafetz et al., 1991; Kano et al., 2007; Kato et al., 2019; Lindqvist, 1994; Osácar et al., 2016). Either directly or indirectly, these parameters ultimately influence the saturation index of the mineral in water (e.g. calcite), thus conditioning the corresponding mineralogical, petrographical and geochemical properties (Arp et al., 2010; Gradziński, 2010; Nehza et al., 2009; Pentecost, 2005).

The most common pattern of lamination is the alternation of two texturally different laminae, the formation of which requires parameters or processes that change periodically (Monty, 1976). Other styles of lamination, such as repetitive or cyclic lamination (Monty, 1976), also require processes that periodically stop or change their characteristics (Suárez-González et al., 2014). Lamina texture reflects the effects of these physical parameters as well as the biological activity on the saturation levels of the mineral (Arp et al., 2005, 2010; Gradziński, 2010). For instance, Casanova (1994) interpreted textural changes in the stromatolite laminae of Pleistocene lakes in the east African rift as a result of seasonal variations in precipitation (runoff) that impacted microbial growth. Generally, large-crystal laminae are linked to precipitation in water with low saturation levels of calcite, for example, during cold temperatures or rainy periods, and small-crystal laminae with higher saturation levels, e.g. during warm temperatures or dry periods (Arenas & Jones, 2017; Arp et al., 2010; Frantz et al., 2014; Kano et al., 2007; Osácar et al., 2016; Woo et al., 2004). Variations in water level, turbidity and velocity or turbulence may also produce differences in lamina texture. Temperature and precipitation, in mid latitude regions, follow seasonal and multi-annual cycles. However, several of these parameters can change periodically and non-periodically, with different frequencies, making it difficult to interpret the temporal significance of lamination (Arenas & Jones, 2017).

The lamina outline or shape is most influenced by the morphology of the microbial components and the formation of distinct structures, as discussed above (Figures 7, 11 and 15C–E). Arenas et al. (2007) described three types of lamination in fluvial oncoids and stromatolites based on lamina shape, clearly dependent on the shape and arrangement style of the microbial bodies. In other cases, the initial shape of the nuclei serves as a template for the lamina shape on a mesoscopic scale (Vázquez-Urbez et al., 2013; Zamarreño et al., 1997).

Stable isotopes (δ^{13}C and δ^{18}O values) have become a useful tool to interpret the environmental and climate significance of the laminae. Precipitation and evaporation are the most satisfactory parameters to explain textural and isotopic variations of the microbialite laminae in hydrologically closed lakes (Arp et al., 2005; Frantz et al., 2014; Woo et al., 2004). This is the case for the stromatolites from the Ebro Basin, in which the light and/or porous laminae record more negative δ^{13}C and δ^{18}O values, attributed to higher ^{12}C inputs and an increased P/E ratio during cool and/or rainy periods. The opposite scenario is proposed for the less negative δ^{13}C and δ^{18}O values of the dark laminae (Martín-Bello et al., 2019b). Correlation between δ^{13}C and δ^{18}O values is very high, although variable through time, and is consistent with the closed basin lake characteristics in units T5 and T6 (Table 2). Similar coupled isotopic and textural relationships were found in the laminae of Eocene stromatolites of the Rife Bed (Tipton Member of the Green River Formation, USA), which formed in saline lake conditions (Frantz et al., 2014), and were interpreted in the same way as in the Ebro Basin. In the Cretaceous lacustrine stromatolites in the Gyeongsang Basin, South-East Korea, Nehza et al. (2009) found an overall trend through lamination, with δ^{18}O values enriched from fibrous calcite towards the succeeding micrite in the Sinyangdong and Hwasan stromatolites. The less negative δ^{18}O values in the micrite were interpreted as representing extensive evaporation of the lake.

In fluvial and hydrological open-lake systems, the effects of evaporation are not as noticeable as in the case of hydrologically closed systems and, therefore, it is possible to estimate or infer variations in water temperature from the δ^{18}O values of calcite (Andrews & Brasier, 2005; Arenas et al., 2015a; Brasier et al., 2010; Dabkowski et al., 2015; Kano et al., 2007; López-Blanco et al., 2016; Osácar et al., 2016). Even with high evaporation, Baringo Lake water remains fresh due to the subsurface water loss through fractures and receives permanent hydrothermal inflows (Owen et al., 2018; Renaut et al., 2002 and references therein). Together these imprint a distinct geochemical composition to the recent microbial deposits, with positive δ^{13}C and δ^{18}O values.

The textural and isotopic comparison of Pleistocene and recent stromatolites in the River Piedra showed a consistent cyclic pattern in both cases and demonstrated that each lamina couplet corresponds to 1 year (Arenas et al.,

2019). The large-crystal laminae in the fossil stromatolites are comparable to the macrocrystalline laminae that occur in the cool-period deposits of the recent stromatolites, and the small-crystal laminae in the fossil specimens are comparable to the warm-period deposits of the recent stromatolites. However, there is not a perfect match. The 7–8.1°C difference calculated between the large-crystal and the small-crystal laminae of the fossil stromatolites is larger than the present difference between summer and winter water temperatures, partially because the large-crystal laminae represent only the coldest record, while the small-crystal laminae represent a longer time span (Arenas et al., 2019). Regardless of this difference, the results are satisfactory and significant enough to interpret similar cyclic variations in the same terms in other laminated microbial records. In other modern fluvial stromatolites, the $\delta^{18}O$ values accurately reflect water temperature differences between laminae formed in different seasons; a record demonstrated to exist in several streams in USA (Chafetz et al., 1991), Japan (Kano et al., 2007; Kawai et al., 2009) and Spain (Osácar et al., 2016). Moreover, trace element composition of successive laminae can also show a rhythmic or trending pattern, which is usually parallel to textural changes. Rodríguez-Berriguete et al. (2018) established different orders of lamination in a recent laminated deposit based on high-resolution geochemical variations, which were consistent with changes in daily to annual water availability.

Clumped isotopes are becoming a useful tool, used in different contexts to determine the temperature at which the carbonate mineral formed (Ghosh et al., 2007; Kele et al., 2015; Petryshyn et al., 2015). However, the results are not yet fully satisfactory or applicable to all cases due to a lack of calibration with natural or experimental examples in different environments and situations (Kele et al., 2015). There are very few works utilising clumped isotopes in laminated microbialites. For example, Petryshyn et al. (2015) studied recent microbialites in Pavilion Lake and Kelly Lake (Canada) and calculated lacustrine water temperature changes obtained from clumped isotopes that were consistent with the measured water temperature changes. However, in the fluvial environment, calculations in natural and experimental conditions have yielded both consistent and inconsistent seasonal temperatures based on clumped isotopes depending on the considered temperature range (Kato et al., 2019; Kele et al., 2015). There is still much to learn in this field from the laminated microbial structures.

3.3.1 | Temporal significance of microbialite lamination

Many of the above-mentioned parameters can produce a cyclic imprint on the textural and geochemical features of the laminae which can be inferred to occur either seasonally or multi-annually. However, the same parameters can vary following periodic and non-periodic frequency processes; the effects of non-periodic processes or parameters can interfere with the periodic ones, thus making it difficult to discern the temporal significance of lamination (Arenas & Jones, 2017).

Several authors, including Monty (1976), Hofmann (1973) and Nehza et al. (2009), among others, have noticed the difficulty in interpreting the temporal significance of stromatolitic lamination, mainly because of its fractal nature, which produces multiple ranks of laminae and of lamina arrangement (Martín-Bello et al., 2019a, 2019b).

Very few works have attempted to date stromatolites through radiogenic isotopic series due to the wide error margins compared with the temporal scale that is intended to be dated. Based on high-resolution sampling for ^{14}C dating, Petryshyn et al. (2012) proposed a lamination frequency (i.e. duration of each pair of laminae) from annual to multi-annual in Holocene Walker Lake stromatolites. However, in most studies, the estimates assume that a given rank of lamination represents a period of time, which is usually supported by the evolution of different parameters, such as the lamina thickness, texture and geochemical values. Periodicity analysis based on variations in thickness, geochemical composition or luminescence can be a helpful tool to link the periods obtained and duration suggested by specific parameters, to probable time cycles.

The parallel cyclic evolution of textural features and $\delta^{13}C$ and/or $\delta^{18}O$ values of consecutive laminae suggests seasonal processes, such as temperature, precipitation and evaporation (Arenas et al., 2015b; Nehza et al., 2009; Woo et al., 2004). However, lower frequency processes could also be responsible for some of these cyclic changes in lacustrine records (Martín-Bello et al., 2019a, 2019b). The periodicity analysis of lamination based on thickness and luminescence of the laminae in lacustrine stromatolites of the early and middle Miocene of the Ebro Basin yielded a range of solar and calendar frequencies, showing that more than one process, with similar or different periods, can intervene to produce lamina periodicity (Pérez-Rivarés et al., 2019), thus making it difficult to differentiate between processes that occur over similar time scales. However, the range in timescales (i.e., periods) is a good fit to the different ranks of laminae differentiated on textural and stable isotope variations (Figures 16 and 17; Martín-Bello et al., 2019b), therefore reinforcing the usefulness of lamination periodicity analysis to gather information on both environment and climate, and indeed to decipher the temporal significance of lamination. Based on periodicity, Pérez-Rivarés et al. (2019) estimated a duration of 120–500 years for specimens 3.5–10 cm thick, thus reinforcing the significance of thick stromatolite successions.

In fluvial records, stromatolite laminae present textural and geochemical variations through time that suit seasonal and sub-seasonal changes, as in the case of recent and Pleistocene deposits in the River Piedra (Arenas et al., 2019; Osácar et al., 2016) and other recent and ancient fluvial records (Andrews & Brasier, 2005; Kano et al., 2007). The thickness and composite nature of seasonal laminae in most recent fluvial stromatolites allows for high-resolution studies (textural, $\delta^{13}C$ and $\delta^{18}O$ values) and these results can be compared with measured and known environmental and climate parameters. In some cases, the resolution is high enough to decipher the climate and temporal significance of the simple laminae or sub-laminae, providing clues to differentiate periodic and non-periodic processes (Arenas & Jones, 2017).

3.3.2 | Microbial mat accretion and sedimentation rates

With regard to lamina accretion, there is no doubt that the sedimentation rates of fluvial and fluvial-open lacustrine stromatolites and oncolites are much higher than those of saline lacustrine microbialites (Arenas et al., 2014a; Pérez-Rivarés et al., 2019). This fact has commonly been explained by the overall high deposition rates in fluvial environments due to calcite saturation levels favoured by intense, mainly mechanical, CO_2 removal. The higher depositional rates of stromatolites with respect to other fluvial carbonate facies has been linked to the preferential growth and faster accretion of microbial mats at sites with fast water flow, which promotes rapid calcite precipitation (Arenas et al., 2014a, 2014b; Arp et al., 2010; Berrendero et al., 2016; Gradziński, 2010).

Results from studies of modern carbonate fluvial systems that have periodically measured sedimentation rates in different facies indicate that the highest rates are recorded by stromatolites, being higher in the warm periods or seasons (at places about twice) than during cooler intervals. Referencing the monitored Iberian Range rivers, calculations of sedimentation rate ranged from 4 to 17 mm/year (Arenas et al., 2015a). Comparable values were obtained by Gradziński (2010) in a field study on several streams of the Carpathian range.

In Pleistocene stromatolites of the River Piedra, assuming each pair of laminae formed in a year, the calculated sedimentation rate was 8.3 mm/year (Arenas et al., 2019). Smaller values were calculated from Pleistocene and Holocene stromatolites in the River Añamaza, with rates of 2.5–2.6 mm/year (Osácar Soriano et al., 2017) (Table 2).

In the Miocene saline stromatolites of the Ebro Basin, sedimentation rate estimates vary between 0.2 and 0.5 mm/year through the several specimens studied, with a mean value of 0.36 mm/year. These rate values are a bit higher than the estimated rates of the other carbonate facies in the lacustrine system (Pérez-Rivarés et al., 2019), but much smaller than the sedimentation rates of recent fluvial stromatolites, which range from 0.4 to 1.7 cm/year (Arenas et al., 2015a; Drysdale & Gillieson, 1997; Gradziński, 2010) (Table 2).

Comparing the sedimentation rates of recent stromatolites measured in several rivers of the Iberian Range (Arenas et al., 2015a) and the calculated rates in the saline carbonate lake stromatolites of the Ebro Basin (Pérez-Rivarés et al., 2019), the growth rates of stromatolites in both environments are higher that the sedimentation rates of the rest of the related carbonate facies. This result prompts discussion and perhaps revision of the idea of slowness of microbial mat accretion in lacustrine and marine carbonate environments.

4 | CONCLUSIONS

The examples of microbialite-bearing sedimentary systems considered in this contribution shed light on the environment and climate (including hydrology) using multi-proxy studies of non-marine laminated microbialites and associated facies at different scales: at megascopic and macroscopic scales (dealing with depositional geometry, architecture and facies models) and at mesoscopic and microscopic scales (dealing with lamination). The larger scales provide information on hydrodynamics, water level changes, depositional architecture, and ultimately lead to facies model proposals. The smaller scales allow for high-resolution interpretation of changing environments and climate through time.

Stromatolites appear to be more frequent in fluvial environments subject to moderate to fast-flowing water than in slow flow conditions. Despite forming over a range of environmental and hydrodynamic conditions, it seems that oncoids develop preferentially in low-slope stretches of sedimentary systems, that is, wide fluvial areas and littoral lacustrine areas, mainly related to low-energy conditions.

Floor topography, hydrology (e.g. water level and hydrodynamics) and occurrence of erosional processes, apart from autocyclic depositional processes, control the geometry of the microbialite deposits and microbialite-bearing deposits in the basin fill. Depending on the structural control, thickness and facies variations may produce highly asymmetrical basin fills.

The interplay of physical and physico-chemical parameters which impact microbial growth is reflected through textural, mineralogical and petrographical features of lamination. It is worth highlighting that the analysis of lamination periodicity has linked stromatolite growth with calendar and solar cycles, thus providing us with clues on the duration of the laminae.

Much remains to be learned about the environmental and climate information recorded in laminated microbial structures in non-marine carbonate systems, in particular at the mesoscopic and microscopic scales.

CONFLICT OF INTEREST

The author has no conflict of interest to declare.

DATA AVAILABILITY STATEMENT

The author confirms that the data supporting the findings of his study are available within the article and its supplementary materials.

ORCID

Concha Arenas-Abad https://orcid.org/0000-0002-4212-0524

REFERENCES

Andrews, J.E. & Brasier, A.T. (2005) Seasonal records of climate change in annually laminated tufas: Short review and future prospects. *Journal of Quaternary Science*, 20, 411–421.

Andrews, J.E., Riding, R. & Dennis, P.F. (1997) The stable isotope record of environmental and climatic signals in modern terrestrial microbial carbonates from Europe. *Palaeogeography, Palaeoclimatology, Palaeoecology*, 129, 171–189.

Anzalone, E., Ferreri, V., Sprovieri, M. & D'Argenio, B. (2007) Travertines as hydrologic archives: The case of the Pontecagnano deposits (southern Italy). *Advances in Water Resources*, 30, 2159–2175.

Arenas, C., Auqué, L., Osácar, C., Sancho, C., Lozano, M.V., Vázquez-Urbez, M. & Pardo. G. (2015a) Current tufa sedimentation in a high discharge river: A comparison with other synchronous tufa records in the Iberian Range (Spain). *Sedimentary Geology*, 325, 132–157.

Arenas, C., Cabrera, L. & Ramos, E. (2003) Fluvial-lacustrine microbialites from the Cala Blanca Formation (Oligocene, Mallorca, western Mediterranean). In: Valero-Garcés, B.L. (ed.) *Limnogeología en España: un tributo a Kerry Kelts*. Biblioteca de Ciencias, 14. Madrid: Consejo Superior Investigaciones Científicas, pp. 119–150.

Arenas, C., Cabrera, L. & Ramos, E. (2007) Sedimentology of tufa facies and continental microbialites from the Palaeogene of Mallorca Island (Spain). *Sedimentary Geology*, 197, 1–27.

Arenas, C., Casanova, J. & Pardo, G. (1997) Stable isotope characterization of the Miocene lacustrine systems of Los Monegros (Ebro Basin, Spain): Palaeogeographic and palaeoclimatic implications. *Palaeogeography, Palaeoclimatology, Palaeoecology*, 128, 133–155.

Arenas, C., Gutiérrez, F., Osácar, C. & Sancho, C. (2000) Sedimentology and geochemistry of fluvial-lacustrine tufa deposits controlled by evaporite solution subsidence in the central Ebro Depression, NE Spain. *Sedimentology*, 47, 883–909.

Arenas, C. & Jones, B. (2017) Temporal and environmental significance of microbial lamination: Insights from Recent fluvial stromatolites in the River Piedra, Spain. *Sedimentology*, 64, 1597–1629.

Arenas, C., Osácar, M.C., Auqué, L.F., Andrews, J.E., Pardo, G., Marca, A., Martín-Bello, L. & Pérez-Rivarés, F.J. (2018) Seasonal temperatures from $\delta^{18}O$ in recent Spanish tufa stromatolites: Equilibrium redux! *Sedimentology*, 65, 1611–1630.

Arenas, C., Osácar, M.C., Auqué, L. & Sancho, C. (2019) Coupling textural and stable-isotope variations in fluvial stromatolites: Comparison of Pleistocene and recent records in NE Spain. *Journal of Palaeogeography*, 8, article number 13.

Arenas, C. & Pardo, G. (1999) Latest Oligocene-Late Miocene lacustrine systems of the north-central part of the Ebro Basin (Spain): Sedimentary facies model and palaeogeographic synthesis. *Palaeogeography, Palaeoclimatology, Palaeoecology*, 151, 127–148.

Arenas, C., Pardo, G. & Casanova, J. (1993) Bacterial stromatolites in lacustrine Miocene deposits of the Ebro Basin (Aragón, Spain). *Bolletino dellà Societá Paleontologica Italiana, Special*, 1, 9–22.

Arenas, C., Piñuela, L. & García-Ramos, J.C. (2015b) Climatic and tectonic controls on carbonate deposition in syn-rift siliciclastic fluvial systems: A case of microbialites and associated facies in the Late Jurassic. *Sedimentology*, 62, 1149–1183.

Arenas, C., Vázquez-Urbez, M., Auqué, L., Sancho, C., Osácar, C. & Pardo, G. (2014a) Intrinsic and extrinsic controls of spatial and temporal variations in modern fluvial tufa sedimentation: A thirteen-year record from a semiarid environment. *Sedimentology*, 61, 90–132.

Arenas, C., Vázquez-Urbez, M., Pardo, G. & Sancho, C. (2014b) Sedimentology and depositional architecture of tufas deposited in stepped fluvial systems of changing slope: Lessons from the Quaternary Añamaza valley (Iberian Range, Spain). *Sedimentology*, 61, 133–171.

Arenas-Abad, C., Vázquez-Urbez, M., Pardo-Tirapu, G. & Sancho-Marcén, C. (2010) Fluvial and associated carbonate deposits. In: Alonso-Zarza, A.M. & Tanner, L.H. (Eds.) *Carbonates in continental settings*. Amsterdam: Elsevier, pp. 133–175.

Arp, G., Bielert, F., Hoffmann, V.E. & Löffler, T. (2005) Palaeoenvironmental significance of lacustrine stromatolites of the Arnstadt Formation ("Steinmergelkeuper", Upper Triassic, N-Germany). *Facies*, 51, 419–441.

Arp, G., Bissett, A., Brinkmann, N., Cousin, S., De Beer, D., Friedl, T. Mohr, K.I., Neu, T.R., Reimer, A., Shiraishi, F., Stackebrandt, E., & Zippel, B. (2010) Tufa-forming biofilms of German karst-water streams: Microorganisms, exopolymers, hydrochemistry and

calcification. *Geological Society of London Special Publications*, *336*, 83–118.

Astibia, H., López Martínez, N., Elorza Zandueta, J.J. & Vicens, E. (2012) Increasing size and abundance of microbialities (oncoids) in connection with the K/T boundary in non-marine environments in the South Central Pyrennees. *Geologica Acta*, *10*, 209–226.

Auqué, L., Arenas, C., Osácar, C., Pardo, G., Sancho, C. & Vázquez-Urbez, M. (2013) Tufa sedimentation in changing hydrological conditions: The River Mesa (Spain). *Geologica Acta*, *11*, 85–102.

Auqué, L., Arenas, C., Osácar, C., Pardo, G., Sancho, C. & Vázquez-Urbez, M. (2014) Current tufa sedimentation in a changing-slope valley: The River Añamaza (Iberian Range, NE Spain). *Sedimentary Geology*, *303*, 26–48.

Awramik, S.M. & Buchheim, H.P. (2009) A giant, Late Archean lake system: The Meentheena Member (Tumbiana Formation; Fortescue Group), Western Australia. *Precambrian Research*, *174*, 215–240.

Berrendero, E., Arenas, C., Mateo, P. & Jones, B. (2016) Cyanobacterial diversity and related sedimentary facies as a function of water flow conditions: Example from the Monasterio de Piedra Natural Park (Spain). *Sedimentary Geology*, *337*, 12–28.

Bouton, A., Vennin, E., Boulle, J., Pace, A., Bourillot, R., Thomazo, C., Brayard, A., Désaubliaux, G., Goslar, T., Yokoyama, Y., Dupraz, C. & Visscher, P.T. (2016) Linking the distribution of microbial deposits from the Great Salt Lake (Utah, USA) to tectonic and climatic processes. *Biogeosciences*, *13*, 5511–5526.

Brasier, A.T., Andrews, J.E., Marca-Bell, A.D. & Dennis, P.F. (2010) Depositional continuity of seasonally laminated tufas: Implications for $\delta^{18}O$ based palaeotemperatures. *Global and Planetary Change*, *71*, 160–167.

Capezzuoli, E., Gandin, A. & Pedley, M. (2014) Decoding tufa and travertine (fresh water carbonates) in the sedimentary record: The state of the art. *Sedimentology*, *61*, 1–21.

Capezzuoli, E., Gandin, A. & Sandrelli, F. (2010) Calcareous tufa as indicators of climatic variability: A case study from southern Tuscany (Italy). *Geological Society, London, Special Publication*, *336*, 263–281.

Carthew, K.D., Taylor, M.P. & Drysdale, R.N. (2006) An environmental model of fluvial tufas in monsoonal tropics, Barkly karst, northern Australia. *Geomorphology*, *73*, 78–100.

Casanova, J. (1994) Stromatolites from the East African Rift: A synopsis. In: Bertrand-Sarfati, J. & Monty, C. (Eds.) *Phanerozoic stromatolites II*. Dordrecht, The Netherlands: Kluwer Academic Publishers, pp. 193–226.

Chafetz, H.S., Utech, N.M. & Fitzmaurice, S.P. (1991) Differences in the $\delta^{18}O$ and $\delta^{13}C$ signatures of seasonal laminae comprising travertine stromatolites. *Journal of Sedimentary Petrology*, *61*, 1015–1028.

Chidsey, T., Vanden Berg, M.D. & Eby, D. (2015) Petrography and characterization of microbial carbonates and associated facies from modern Great Salt Lake and Uinta Basin's Eocene Green River Formation in Utah, USA. In: Bosence, D.W.J., Gibbons, K.A., Le Heron, D.P., Morgan, W.A., Pritchard, T. & Vining, B.A. (Eds.) *Microbial carbonates in space and time: Implications for global exploration and production. Geological Society, London, Special Publications*, *418*(1), 261–286.

Dabkowski, J., Royle, S.H., Antoine, P., Marca-Bell, A. & Andrews, J.E. (2015) High resolution $\delta^{18}O$ seasonality record in a French Eemian tufa stromatolite (Caours, Somme Basin). *Palaeogeography, Palaeoclimatology, Palaeoecology*, *438*, 277–284.

Della Porta, G. (2015) Carbonate build-ups in lacustrine, hydrothermal and fluvial settings: Comparing depositional geometry, fabric types and geochemical signature. In: Bosence, D.W.J., Gibbons, K.A., Le Heron, D.P., Morgan, W.A., Pritchard, T. & Vining, B.A. (Eds.), *Microbial carbonates in space and time: Implications for global exploration and production. Geological Society, London, Special Publications 418*, 17–68.

Deschamps, R., Rohais, S., Hamon, Y. & Gasparrini, M. (2020) Dynamic of a lacustrine sedimentary system during late rifting at the Cretaceous-Palaeocene transition: Example of the Yacoraite Formation, Salta Basin, Argentina. *The Depositional Record*, *6*, 490–523.

Drysdale, R.N. & Gillieson, D. (1997) Micro-erosion meter measurements of travertine deposition rates: A case study from Louie Creek, northwest Queensland, Australia. *Earth Surface Processes and Landforms*, *22*, 1037–1051.

Durán, J.J. (1989) Geocronología de los depoósitos asociados al karst en España. In: Durán, J.J. & López-Martínez, J. (Eds), *El karst en España*. Sociedad Española de Geomorfología, Monograph 4. Madrid: Sociedad Española de Geomorfología, pp. 243–256.

Fischer, A.G. & Herbert, T.D. (1986) Stratification rhythms: Italo-American studies in the Umbrian facies. *Memorie della Società Geologica Italiana*, *31*, 45–51.

Ford, T.D. & Pedley, H.M. (1996) A review of tufa and travertine deposits of the world. *Earth Science Reviews*, *41*(3–4), 17–175.

Frantz, C.M., Petryshyn, V.A., Marenco, P.J., Tripati, A., Berelson, W.M. & Corsetti, F.A. (2014) Dramatic local environmental change during the Early Eocene Climatic Optimum detected using high resolution chemical analyses of Green River Formation stromatolites. *Palaeogeography, Palaeoclimatology, Palaeoecology*, *405*, 1–15.

Gallois, A., Bosence, D. & Burguess, P.M. (2018) Brackish to hypersaline facies in lacustrine carbonates: Purbeck Limestone Group, Upper Jurassic-Lower Cretaceous, Wessex Basin, Dorset, UK. *Facies*, *64*, 42. https://doi.org/10.1007/s10347-018-0525-4

García-García, F., Pla-Pueyo, S., Nieto, L.M. & Viseras, C. (2014) Sedimentology of geomorphologically controlled Quaternary tufas in a valley in southern Spain. *Facies*, *60*, 53–72.

Ghosh, P., Eiler, J., Campana, S.E. & Feeney, R.F. (2007) Calibration of the carbonate 'clumped isotope' paleothermometer for otoliths. *Geochimica et Cosmochimica Acta*, *71*, 2736–2744.

Gierlowski-Kordesch, E.H. (2010) Lacustrine carbonates. In: Alonso-Zarza, A.M. & Tanner, L.H. (Eds.), *Carbonates in continental settings*, Developments in Sedimentology 61. Amsterdam: Elsevier, pp. 1–101.

Gradziński, M. (2010) Factors controlling growth of modern tufa: Results of a field experiment. *Geological Society of London Special Publications*, *336*, 143–191.

Graf, J.W., Carroll, A.R. & Smith, M.E. (2015) Lacustrine sedimentology, stratigraphy and stable isotope geochemistry of the Tipton Member of the Green River Formation. In: Smith, M.E. & Carroll, A.R. (Eds.), *Stratigraphy and paleolimnology of the Green River Formation, Western USA*. Syntheses in Limnogeology 1. Dordrecht: Springer, pp. 31–60.

Hägele, D., Leinfelder, R., Grau, J., Burmeister, E.G. & Struck, U. (2006) Oncoids from the river Alz (southern Germany): Tiny ecosystems in a phosphorus-limited environment. *Palaeogeography, Palaeoclimatology, Palaeoecology*, *237*, 378–395.

Han, Z., Zhang, X., Chi, N., Han, M., Woo, J., Lee, H.S. & Chen, J. (2014) Cambrian oncoids and other microbial-related grains on the

North China Platform. *Carbonates and Evaporites*, *30*, 373–386. https://doi.org/10.1007/s13146-014-0209-2

Harris, P.M., Ellis, J. & Purkis, S.J. (2013) Assessing the extent of carbonate deposition in early rift settings. *AAPG Bulletin*, *97*(1), 27–60.

Hofmann, H.J. (1973) Stromatolites: Characteristics and utility. *Earth-Science Reviews*, *9*, 339–373.

Jones, B. & Renaut, R.W. (1994) Crystal fabrics and microbiota in large pisoliths from Laguna Pastos Grandes, Bolivia. *Sedimentology*, *41*, 1171–1202.

Kano, A., Hagiwara, R., Kawai, T., Hori, M. & Matsuoka, J. (2007) Climatic conditions and hydrological change recorded in a high-resolution stable-isotope profile of a recent laminated tufa on a subtropical island, southern Japan. *Journal of Sedimentary Research*, *77*, 59–67.

Kato, H., Amekawa, S., Kano, A., Mori, T., Kuwahara, Y. & Quade, J. (2019) Seasonal temperature changes obtained from carbonate clumped isotopes of annually laminated tufas from Japan: Discrepancy between natural and synthetic calcites. *Geochimica et Cosmochimica Acta*, *244*, 548–564.

Kawai, T., Kano, A. & Hori, M. (2009) Geochemical and hydrological controls on biannual lamination of tufa deposits. *Sedimentary Geology*, *213*, 41–50.

Kele, S., Breitenbach, S.F.M., Capezzuoli, E., Meckler, A.N., Ziegler, M., Millan, I.M. Kluge, T., Deák, J., Hanselmann, K., John, C. M., Yan, H., Liu, Z. & Bernasconi S. M. (2015) Temperature dependence of oxygen- and clumped isotope fractionation in carbonates: A study of travertines and tufas in the 6–95ºC temperature range. *Geochimica et Cosmochimica Acta*, *168*, 172–192.

Kelts, K. & Talbot, M.R. (1990) Lacustrine Carbonates as geochemical archives of environmental change and biotic/abiotic interactions. In: Tilzer, M.M. & Serruya, C. (Eds.) *Large lakes: Ecological structure and function*. Berlin: Springer-Verlag, pp. 288–315.

Leinfelder, R.R. (1985) Cyanophyte calcification morphotypes and depositional environments (Alenquer oncolite, Upper Kimmeridgian? Portugal). *Facies*, *12*, 253–274.

Lettéron, A., Hamon, Y., Fournier, F., Séranne, M., Pellenard, P. & Joseph, P. (2018) Reconstruction of a saline, lacustrine carbonate system (Priabonian, St-Chaptes Basin, SE France): Depositional models, paleogeographic and paleoclimatic implications. *Sedimentary Geology*, *367*, 20–47.

Lindqvist, J.K. (1994) Lacustrine stromatolites and oncoids. Manuherikia Group (Miocene), New Zealand. In: Bertrand-Sarfati, J. & Monty, C. (Eds.) *Phanerozoic stromatolites II*. Dordrecht, The Netherlands: Kluwer Academic Publishers, pp. 227–254.

López-Blanco, C., Andrews, J., Dennis, P., Rosa, M. & Vicente, E. (2016) North Atlantic Oscillation recorded in carbonate δ^{18}O signature from Lagunillo del Tejo (Spain). *Palaeogeography, Palaeoclimatology, Palaeoecology*, *441*, 882–889.

Mäcker, H. (1997) Upper Cretaceous and Lower Tertiary brackish to freshwater oncoids and stromatolites of the Garumnian facies in the Àger Basin (Central Southern Pyrenees, Spain). *Facies*, *36*, 246–249.

Martín-Bello, L.A., Abad, C. & Jones, B. (2019a) Lacustrine stromatolites: Useful structures for environmental interpretation – An example from the Miocene Ebro Basin. *Sedimentology*, *66*, 2098–2133.

Martín-Bello, L., Arenas, C., Andrews, J., Alonso-Zarza, A.M. & Marca, A. (2019b) Multi-scale records of climate change in lacustrine stromatolites: Insights from the Miocene Ebro Basin. *Palaeogeography, Palaeoclimatology, Palaeoecology*, *530*, 312–329.

Martini, I. & Capezzuoli, E. (2014) Interdigitated fluvial clastic deposits and calcareous tufa testifying an uplift of the catchment area: An example from the Pianizzoli area (southern Tuscany, Italy). *Sedimentary Geology*, *299*, 60–73.

Meléndez, N. & Gómez-Fernández, J.C. (2000) Continental deposits of the Eastern Cameros Basin (Northern Spain) during Tithonian-Berriasian Time. In: Gierlowski-Kordesch, E.H. & Kelts, K.R. (eds) *Lake basins through space and time. AAPG Studies in Geology 6*, 263–278.

Monty, C.L.V. (1976) The origin and development of cryptalgal fabrics. In: Walter, M.R. (Ed.) *Stromatolites*. Amsterdam: Elsevier, pp. 193–249.

Muniz, M.C. & Bosence, D.W.J. (2015) Pre-salt microbialites from the Campos Basin (offshore Brazil): Image log facies, facies model and cyclicity in lacustrine carbonates. In: Bosence, D.W.J., Gibbons, K.A., Le Heron, D.P., Morgan, W.A., Pritchard, T. & Vining, B.A. (Eds.) *Microbial carbonates in space and time: Implications for global exploration and production. Geological Society London, Special Publication*, *418*, 221–242.

Muñoz, A., Arenas, C., González, A., Luzón, A., Pardo, G., Pérez, A. & Villena, J. (2002) Ebro Basin (Northeastern Spain). In: Gibbons, W. & Moreno, T. (Eds.), *The geology of Spain. Geological Society of London*, 301–309.

Nehza, O., Woo, K.S. & Lee, K.C. (2009) Combined textural and stable isotopic data as proxies for the mid–Cretaceous paleoclimate: A case study of lacustrine stromatolites in the Gyeongsang Basin, SE Korea. *Sedimentary Geology*, *214*, 85–99.

Nickel, E. (1983) Environmental significance of freshwater oncoids, Eocene Guara Formation, Southern Pyrenees, Spain. In: Peryt, T.M. (Ed.) *Coated grains*. Berlin: Springer, pp. 308–329.

Ordóñez, S., Cuevas, J., Benavente, D. & García del Cura, M.A. (2016) Architecture of Pleistocene fluvial tufa systems associated with waterfalls: El Salt (Alcoy, Spain). *Geogaceta*, *59*, 7–10.

Ordóñez, S. & García del Cura, M.A. (1983) Recent and tertiary fluvial carbonates in Central Spain. In: Collinson, J.D. & Lewin, J. (Eds.) *Ancient and modern fluvial systems. International Association of Sedimentologists, Special Publication*, *6*, 485–497.

Ordóñez, S., González Martín, J.A., García del Cura, M.A. & Pedley, H.M. (2005) Temperate and semi-arid tufas in Pleistocene to Recent fluvial barrage system in the Mediterranean area: The Ruidera Lakes Natural Park (Central Spain). *Geomorphology*, *69*, 332–350.

Osácar, C., Arenas, C., Auqué, L., Sancho, C., Pardo, G. & Vázquez-Urbez, M. (2016) Discerning the interactions between environmental parameters reflected in δ^{13}C and δ^{18}O of recent fluvial tufas: Lessons from a Mediterranean climate region. *Sedimentary Geology*, *345*, 126–144.

Osácar Soriano, M.C., Arenas Abad, C., Sancho Marcén, C., Pardo Tirapu, G. & Martín Bello, L. (2017) Stable-isotope changes in tufa stromatolites of the Quaternary Añamaza fluvial system (Iberian Ranges, Spain). *Geogaceta*, *61*, 167–170.

Owen, R.B., Renaut, R.W. & Lowenstein, T.K. (2018) Spatial and temporal geochemical variability in lacustrine sedimentation in the East African Rift System: Evidence from the Kenya Rift and regional analyses. *Sedimentology*, *65*, 1697–1730.

Özkul, M., Görgöz, A., Kele, S., Baykara, M.O., Shen, C.C., Chang, Y.W., Kaya, A., Hançer, M., Aratman, C., Akin, T. & Örü, Z. (2014) Sedimentological and geochemical characteristics of a fluvial travertine: A case from the eastern Mediterranean region. *Sedimentology*, *61*, 291–318.

Parcerisa, D., Gómez-Gras, D. & Martín-Martín, J.D. (2006) Calcretes, oncolites, and lacustrine limestones in Upper Oligocene alluvial fans of the Montgat area (Catalan Coastal Ranges, Spain). In: Alonso-Zarza, A.M. & Tanner, L.H. (Eds.), *Paleoenvironmental record and applications of calcretes and palustrine carbonates. Geological Society of America Special Paper 416*, 105–118.

Pardo, G., Arenas, C., González, A., Luzón, A., Muñoz, A., Pérez, A., Pérez-Rivarés, F.J., Vázquez-Urbez, M. & Villena, J. (2004) La Cuenca del Ebro. In: Vera, J.A. (Ed.) *Geología de España*. Madrid: SGE-IGME, pp. 533–543.

Pedley, H.M. (1990) Classification and environmental models of cool freshwater tufas. *Sedimentary Geology*, 68, 143–154.

Pedley, M. (2009) Tufas and travertines of the Mediterranean region: A testing ground for freshwater carbonate concepts and developments. *Sedimentology*, 56, 221–246.

Pentecost, A. (2005) *Travertine*. Berlin: Springer-Verlag, 445 pp.

Pérez-Rivarés, F.J. (2016) Studio magnetoestratigráfico del Mioceno del sector central de la Cuenca del Ebro: Cronología, correlación y análisis de la ciclicidad sedimentaria. PhD Thesis. Universidad de. Zaragoza, 281 pp. https://zaguan.unizar.es/record/79504?ln=en

Pérez-Rivarés, F.J., Arenas, C., Pardo, G. & Garcés, M. (2018) Temporal aspects of genetic stratigraphic units in continental sedimentary basins: Examples from the Ebro Basin, Spain. *Earth Science Reviews*, 178, 136–153.

Pérez-Rivarés, J., Martín-Bello, L. & Arenas-Abad, C. (2019) Periodicity in stromatolitic lamination: A potential record of ENSO, NAO and SUNSPOT. The Miocene lacustrine record in the Ebro Basin. *Spain. Sedimentary Geology*, 390, 83–99.

Petryshyn, V.A., Corsetti, F.A., Berelson, W.M., Beaumont, W. & Lund, S.P. (2012) Stromatolite lamination frequency, Walker Lake, Nevada: Implications for stromatolites as biosignatures. *Geology*, 40(6), 499–502.

Petryshyn, V.A., Lim, D., Laval, B.L., Brady, A., Slater, G. & Tripati, A.K. (2015) Reconstruction of limnology and microbialite formation conditions from carbonate clumped isotope thermometry. *Geobiology*, 13(1), 53–67.

Pietras, J.T. & Carroll, A.R. (2006) High-resolution stratigraphy of an underfilled lake basin: Wilkins Peak member, Eocene Green River Formation, Wyoming, USA. *Journal of Sedimentary Research*, 76, 1197–1214.

Platt, N.H. & Wright, V.P. (1991) Lacustrine carbonates: Facies models, facies distributions and hydrocarbon aspects. *Special Publications of the International Association of Sedimentologists*, 13, 57–74.

Renaut, R., Jones, B., Tiercelin, J. & Tarits, C. (2002) Sublacustrine precipitation of hydrothermal silica in rift lakes: Evidence from Lake Baringo, central Kenya Rift Valley. *Sedimentary Geology*, 148, 235–257.

Riding, R. (2000) Microbial carbonates: The geological record of calcified bacterial-algal mats and biofilms. *Sedimentology*, 47, 179–214.

Riding, R. (2011) Microbialites, stromatolites and thrombolites. In: Reitner, J. & Thiel, V. (Eds.) *Encyclopedia of geobiology*. Berlin: Springer, pp. 635–654.

Roche, A., Vennin, E., Bouton, A., Olivier, N., Wattinne, A., Bundeleva, I., Deconinck, J.F., Virgone, A., Gaucher, E.C. & Visscher, P.T. (2018) Oligo-Miocene lacustrine microbial and metazoan buildups from the Limagne Basin (French Massif Central). *Palaeogeography, Palaeoclimatology, Palaeoecology*, 504, 34–59.

Rodríguez-Berriguete, A., Alonso-Zarza, A.M., Martín-García, R. & Cabrera, M.C. (2018) Sedimentology and geochemistry of a human-induced tufa deposit: Implications for palaeoclimatic research. *Sedimentology*, 65, 2253–2277.

Sancho, C., Arenas, C., Vázquez-Urbez, M., Pardo, G., Lozano, M.V., Peña-Monné, J.L., Hellstrom, J., Ortiz, J.E., Osácar, M.C., Auqué, L. & Torres, T. (2015) Climatic implications of the Quaternary fluvial tufa record in the NE Iberian Peninsula over the last 500 ka. *Quaternay Research*, 84(3), 398–414.

Santos Bueno, N., Arenas Abad, C. & Gil Imaz, A. (2019) Miocene syntectonic fluvial and lacustrine sedimentation linked to a fault-parallel buttress syncline in the Nigüella sector (NW Iberian Range). *Estudios Geológicos*, 75(1), e089. 10.3989/egeol.43377.507

Scott, J.J. & Smith, M.E. (2015) Trace Fossils of the Eocene Green River Lake Basins, Wyoming, Utah, and Colorado. In: Smith, M.E. & Carroll, A.R. (Eds), *Stratigraphy and Paleolimnology of the Green River Formation, Western USA*. Syntheses in Limnogeology, 1. Dordrecht: Springer, pp. 313–350.

Seard, C., Camoin, G., Rouchy, J.M. & Virgone, A. (2013) Composition, structure and evolution of a lacustrine carbonate margin dominated by microbialites: Case study from the Green River formation (Eocene; Wyoming, USA). *Palaeogeography, Palaeoclimatology, Palaeoecology*, 381–382, 128–144.

Smith, M.E., Carroll, A.R. & Scott, J.J. (2015) Stratigraphic expression of climate, tectonism, and geomorphic forcing in an underfilled lake basin: Wilkins Peak Member of the Green River Formation. In: Smith, M.E. & Carroll, A.R. (Eds.), *Stratigraphy and paleolimnology of the Green River Formation, Western USA*. Syntheses in Limnogeology, 1. Dordrecht: Springer, pp. 61–102.

Smoot, J.P. (1983) Depositional subenvironments in an arid closed basin: The Wilkins Peak Member of the Green River Formation (Eocene), Wyoming, USA. *Sedimentology*, 30, 801–827.

Storrie-Lombardi, M.C. & Awramik, S.M. (2006) A sideways view of stromatolites: Complexity metrics for stromatolite laminae. Proc. SPIE Instruments, Methods, Mission. Astrobiol. IX 6309, 63090P. https://doi.org/10.1117/12.679869

Suárez-González, P., Quijada, I.E., Benito, M.I., Mas, R., Merinero, R. & Riding, R. (2014) Origin and significance of lamination in Lower Cretaceous stromatolites and proposal for a quantitative approach. *Sedimentary Geology*, 300, 11–27.

Talanda, M., Bajdek, P., Niedzwiedzki, G. & Sulej, T. (2017) Upper Triassic freshwater oncoids from Silesia (southern Poland) and their microfossil biota. *Neues Jahrbuch für Geologie und Paläontologie - Abhandlungen*, 284(1), 43–56.

Tang, D., Shi, X. & Jiang, G. (2014) Sunspot cycles recorded in Mesoproterozoic carbonate biolaminites. *Precambrian Research*, 248, 1–16.

Toker, E. (2017) Quaternary fluvial tufas of Sarıkavak area, southwestern Turkey: Facies and depositional systems. *Quaternary International, Non-Marine Carbonates, Special Issue*, 437, 37–50.

Tosti, F. & Riding, R. (2017) Fine-grained agglutinated elongate columnar stromatolites: Tieling Formation, ca 1420 Ma, North China. *Sedimentology*, 64, 871–902.

Vázquez-Urbez, M. (2008) Caracterización y significado ambiental de depósitos tobáceos neógenos en la Cuenca del Ebro. Comparación con ambientes cuaternarios. PhD Thesis, Universidad de Zaragoza, Zaragoza. https://zaguan.unizar.es/record/2057

Vázquez-Urbez, M., Arenas, C. & Pardo, G. (2012) A sedimentary facies model for stepped, fluvial tufa systems in the Iberian Range (Spain): The Quaternary Piedra and Mesa valleys. *Sedimentology*, *59*, 502–526.

Vázquez-Urbez, M., Arenas, C., Pardo, G. & Pérez-Rivares, J. (2013) The effect of drainage reorganization and climate on the sedimentologic evolution of intermontane lake systems: The final fill stage of the Tertiary Ebro Basin (Spain). *Journal of Sedimentary Research*, *83*, 562–590.

Vázquez-Urbez, M., Pardo, G., Arenas, C. & Sancho, C. (2011) Fluvial diffluence episodes reflected in the Pleistocene tufa deposits of the river Piedra (Iberian range, NE Spain). *Geomorphology*, *125*(1), 1–10.

Vennin, E., Bouton, A., Bourillot, R., Pace, A., Roche, A., Brayard, A., Thomazo, C., Virgone, A., Eric C. Gaucher, E.C., Desaubliaux, G. & Visscher, P.T. (2019) The lacustrine microbial carbonate factory of the successive Lake Bonneville and Great Salt Lake, Utah, USA. *Sedimentology*, *66*(1), 165–204.

Vera, J.A. (2004, Ed.). Geología de España. Madrid: SGE-IGME.

Verrecchia, E.P., Freytet, P., Julien, J. & Baltzer, F. (1997) The unusual hydrodynamical behaviour of freshwater oncolites. *Sedimentary Geology*, *113*(3–4), 225–243.

Violante, C., Ferreri, V., D'Argenio, B. & Golubic, S. (1994) Quaternary travertines at Rocchetta a Volturno (Isernia, central Italy). Facies analysis and sedimentary model of an organogenic carbonate system. Excursion A1, 15th lAS Regional Meeting, Ischia, ltaly, 21 pp.

Woo, K.S., Khim, B.K., Yoon, H.S. & Lee, K.C. (2004) Cretaceous lacustrine stromatolites in the Gyeongsang Basin (Korea): Records of cyclic change in paleohydrological condition. *Geoscience Journal*, *8*, 179–184.

Zamarreño, I., Anadón, P. & Utrilla, R. (1997) Sedimentology and isotopic composition of Upper Palaeocene to Eocene non-marine stromatolites, eastern Ebro Basin, NE Spain. *Sedimentology*, *44*, 159–176.

Zeng, L.Q., Yi, H.S., Xia, G.Q., Simon, K., Heim, C. & Arp, G. (2019) Palaeoenvironmental setting of lacustrine stromatolites in the Miocene Wudaoliang Group, northern Tibetan Plateau. *Journal of Palaeogeography*, *8*, 18. https://doi.org/10.1186/s42501-019-0033-7